Seismic elastic double-beam characterization of faults and fractures for CO_2 storage site selection

Project Number: DE-FE0032063

Project start date: July 1, 2021

Yingcai Zheng

University of Houston

U.S. Department of Energy
National Energy Technology Laboratory
2022 Project Review Meeting, Pittsburgh
08/16/2020 11am

Teams

- University of Houston
  - Yingcai Zheng (PI)
  - Jake Parsons (graduate student)
  - Sharmila Appini (graduate student)
  - Yuesu Jin (graduate student)
  - Hao Hu (postdoc)

- Los Alamos National Laboratory
  - Lianjie Huang (Co-PI)
  - David Li (graduate research assistant)
  - Neala Creasy (postdoc)

- Vecta Oil and Gas, Ltd.
  - Bryan DeVault (President/CEO; Co-PI)
  - Gulia Popov

FINANCIAL ASSISTANCE
FUNDING OPPORTUNITY ANNOUNCEMENT

Department of Energy (DOE)
Office of Fossil Energy (FE)

EMERGING CO_2 STORAGE TECHNOLOGIES: OPTIMIZING PERFORMANCE THROUGH MINIMIZATION OF SEISMICITY RISKS AND MONITORING CAPROCK INTEGRITY

Funding Opportunity Announcement (FOA) Number: DE-FOA-0002401

Announcement Type: Amendment 1[1]

CFDA Number: 81.089

EMERGING CO_2 STORAGE TECHNOLOGIES: OPTIMIZING PERFORMANCE THROUGH MINIMIZATION OF SEISMICITY RISKS AND MONITORING CAPROCK INTEGRITY

Funding Opportunity Announcement (FOA) Number: DE-FOA-0002401

AOI 1a - Fault Detection, Characterization, and Hazard Assessment.

No field work. Novel method development. Final deliverable: a software package for subsurface analysis for Gigatonne storage scenarios.

Goals and Objectives for Gigatonne injection

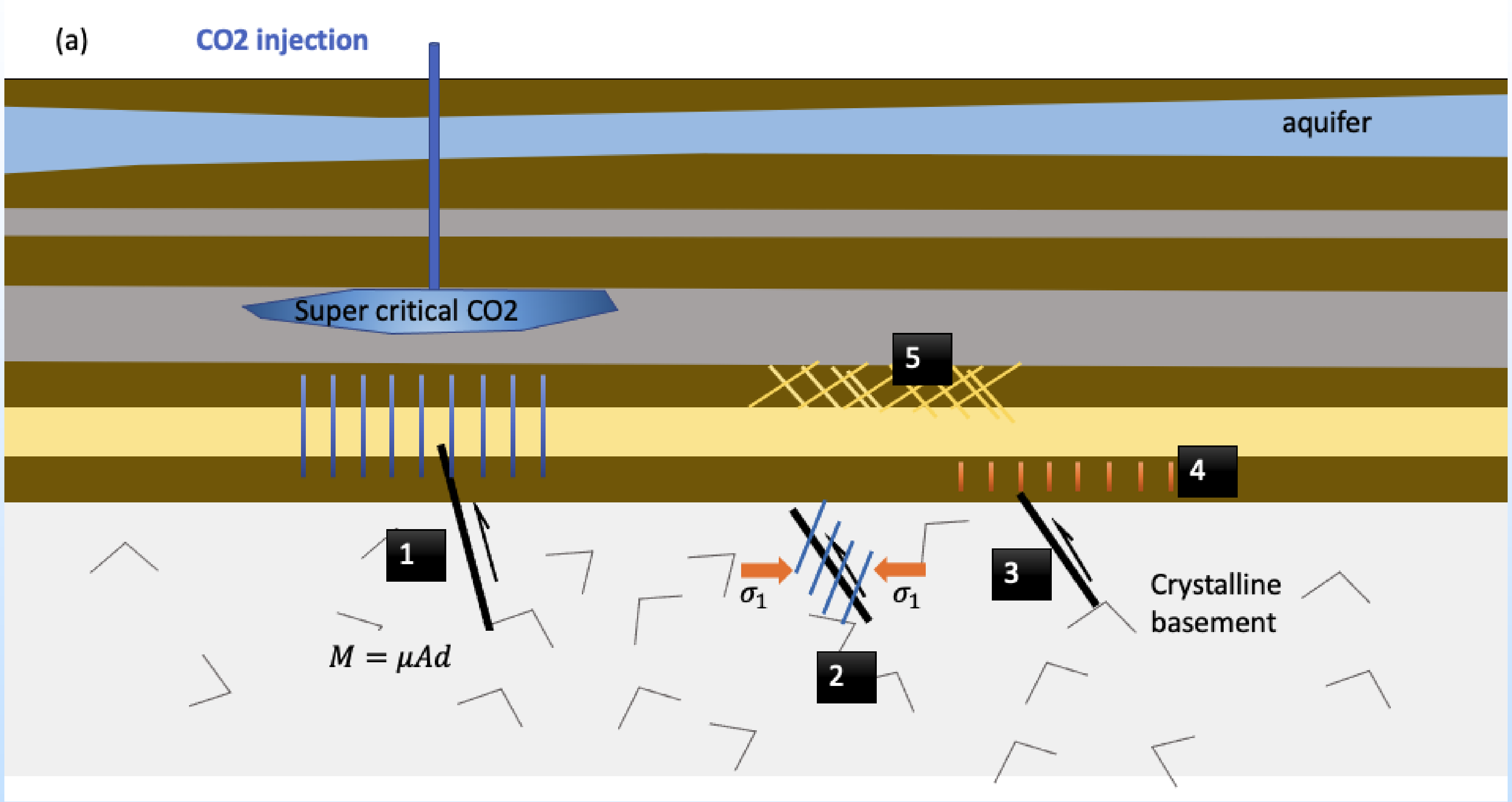

Methodology

- Develop 9-component (9C) elastic double-beam method for small-scale fracture characterization (self validating)
- Develop large-scale fault detection method
- Synthesis:
  - fractures/faults in sedimentary layers and basement;
  - Stress
  - Estimating earthquake hazards
  - Estimating fluid pathways to basement faults
- Field data test: 9C seismic dataset from Wolf Springs in Central Montana

Objectives budget periods (BP)

- **<u>BP 1.</u>** Fault detection and fracture characterization in the basement using <u>synthetic</u> 9C surface seismic data (Year-1)
- **<u>BP 2.</u>** Fault detection and fracture characterization in the basement using <u>field</u> 9C surface seismic data (Year-2)
- **<u>BP 3.</u>** Determination of fault stress state and fault activation potential (Year-3)

Task/Subtask Breakdown

Task 2.0 - Fault detection and fracture characterization in the basement using synthetic 9C surface seismic data

This task will be in Year-1 which is the budget period 1. The work will focus on synthetic dataset based on a model with dimensions similar to the Wolf Springs field data.

- Subtask 2.1 – (UH/LANL/Vecta) Model building based on central Montana (M1-M3): Build a 3D elastic model using the Wolf Springs field geometry.
- Subtask 2.2 – (UH) Multicomponent synthetic seismic data modeling (M4-M6): Using the model and the locations of the sources and receivers in the field data, UH will run their elastic finite-difference code to generate the synthetic datasets. The computation will be done on PI's group cluster.
- Subtask 2.3 – (LANL) Migration imaging (M7-M9): LANL will conduct P-P, P-S, S-P, and S-S imaging on the synthetic dataset.
- Subtask 2.4 – (LANL) Machine learning fault detection (M10-M12): LANL will detect faults on P-P, P-S, S-P, and S-S images of the synthetic dataset.
- Subtask 2.5 – (UH) Fracture characterization using elastic double beam (M10-M12)

Roadmap

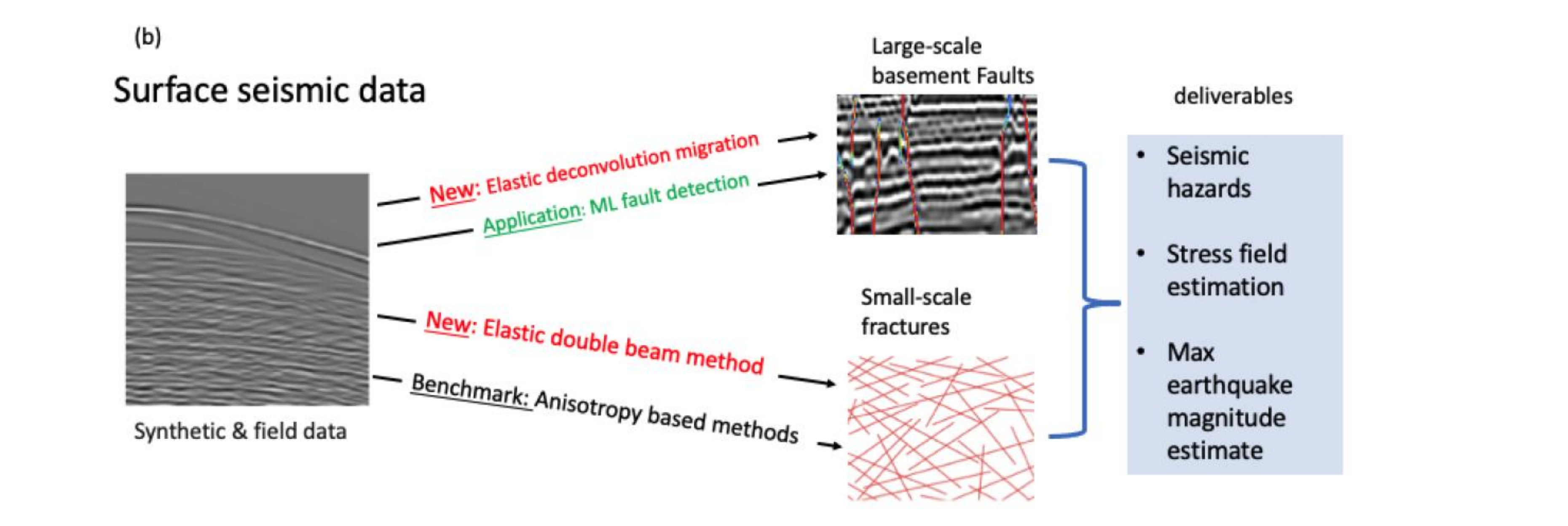

(b)
Surface seismic data
Synthetic & field data
New: Elastic deconvolution migration
Application: ML fault detection
New: Elastic double beam method
Benchmark: Anisotropy based methods
Large-scale
basement Faults
Small-scale
fractures
deliverables
• Seismic hazards
• Stress field estimation
• Max earthquake magnitude estimate

Why another method for fracture characterization?

- Can seismic migration see the small-scale fractures?

- No.

Motivational example: fractures are hard to see

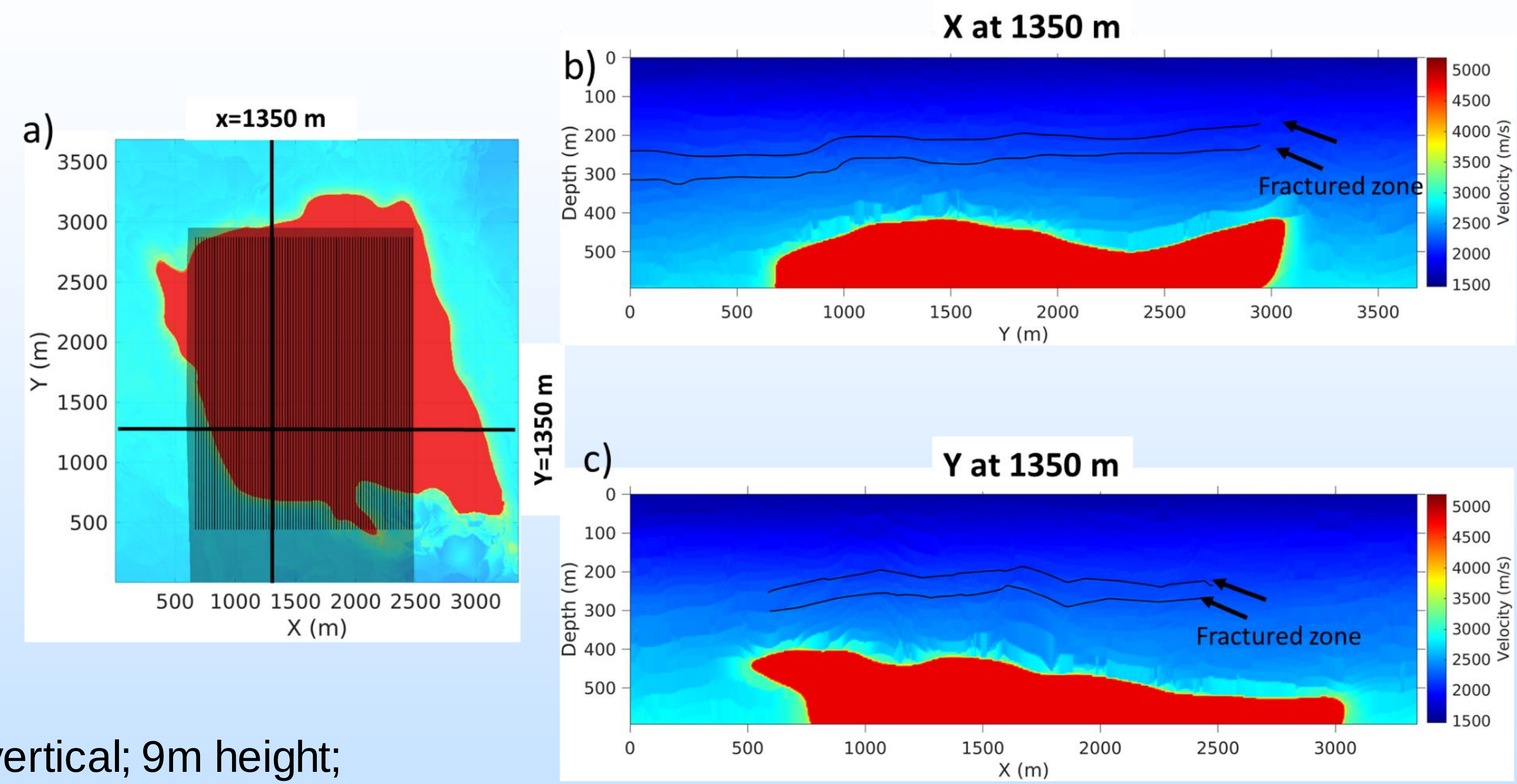

Fractures: vertical; 9m height;
fracture compliance 1e-10 m/Pa

Finite difference modeling: Coates and Schoenberg (1995)

Hard to see fractures in traditional seismic migrated images

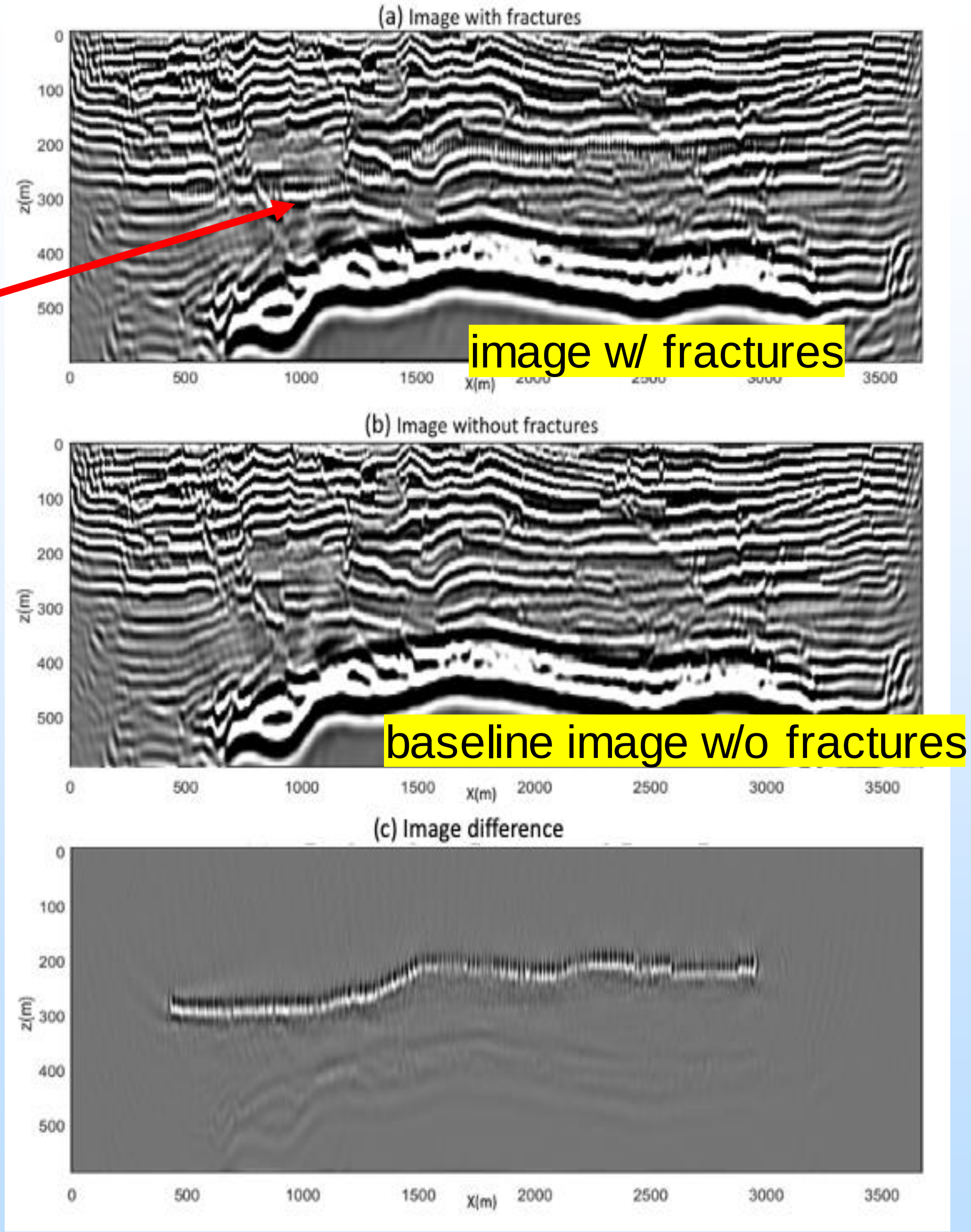

How does the seismic double-beam method characterize small-scale fractures

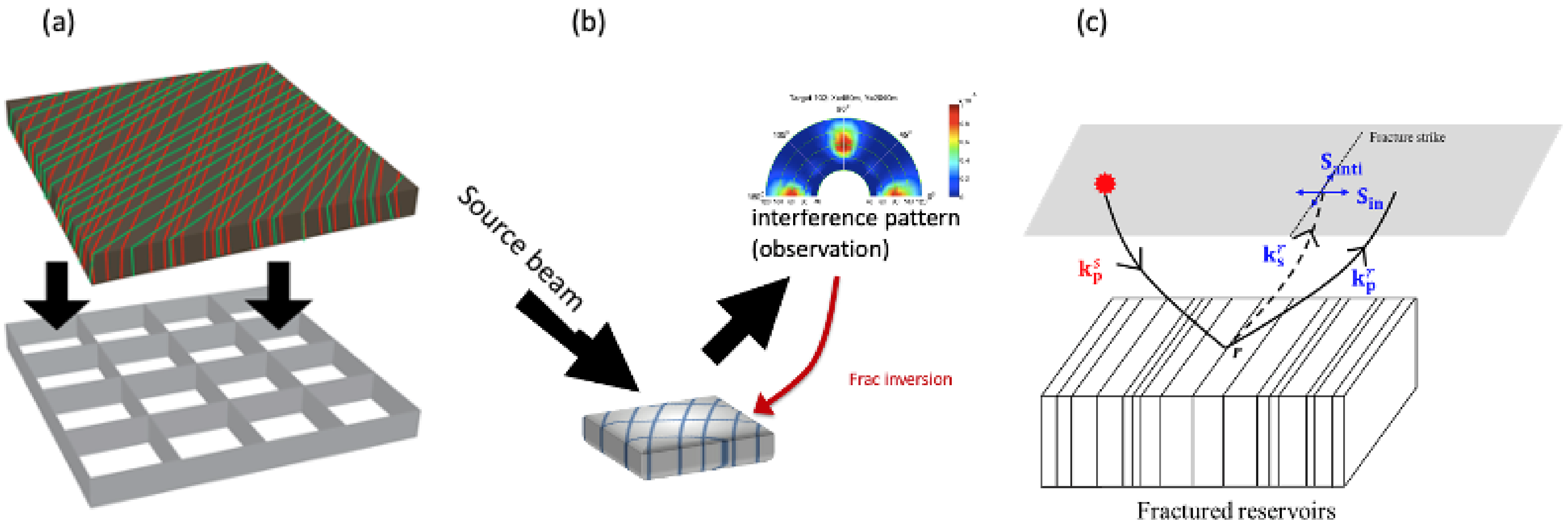

(a)
(b)
(c)
Source beam
interference pattern
(observation)
Frac inversion
Fracture strike
S_{anti}
S_{in}
k_p^s
k_s^r
k_p^r
r
Fractured reservoirs

From point sources to localized wave packet

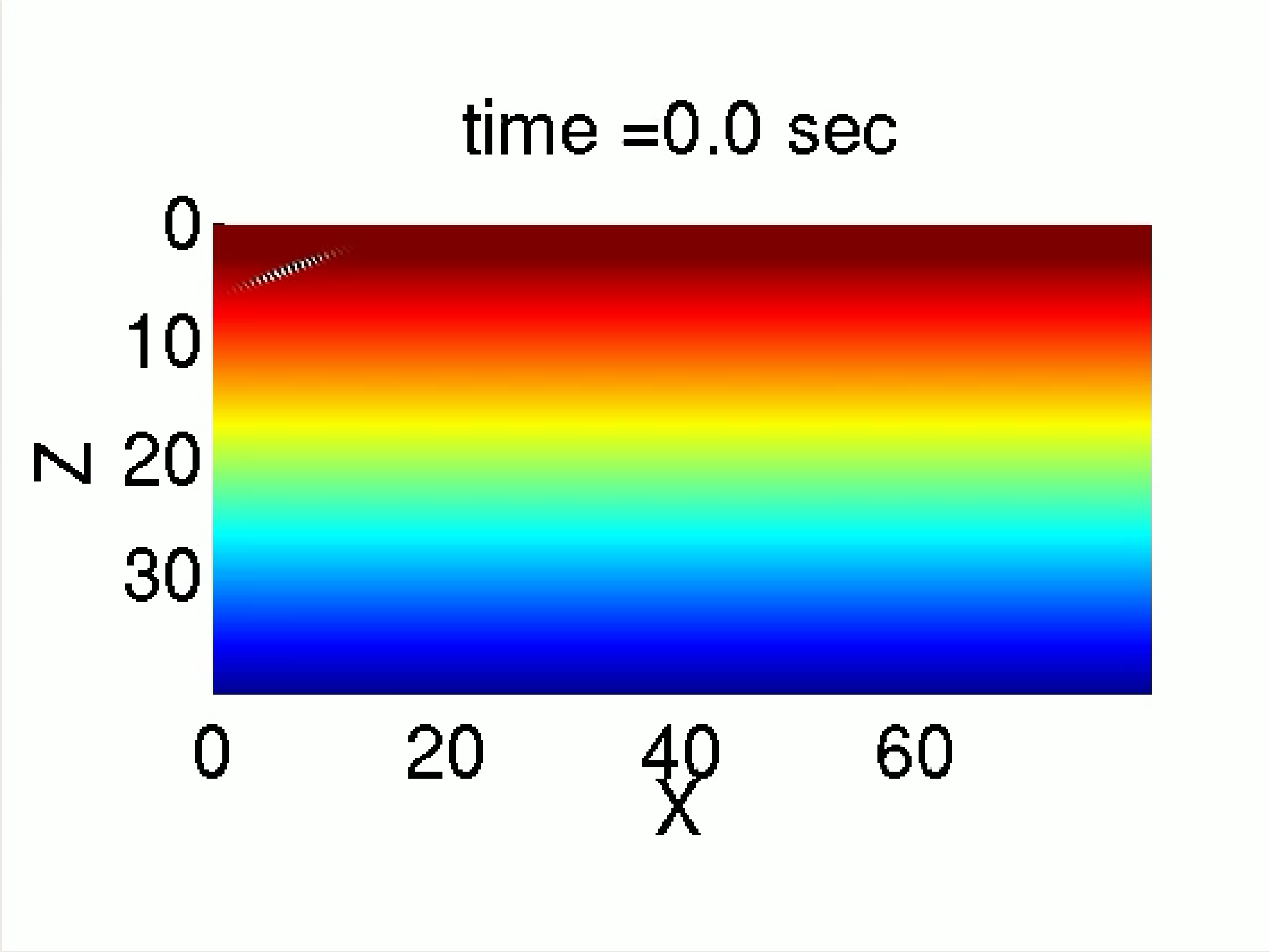

From point sources to localized wave packet

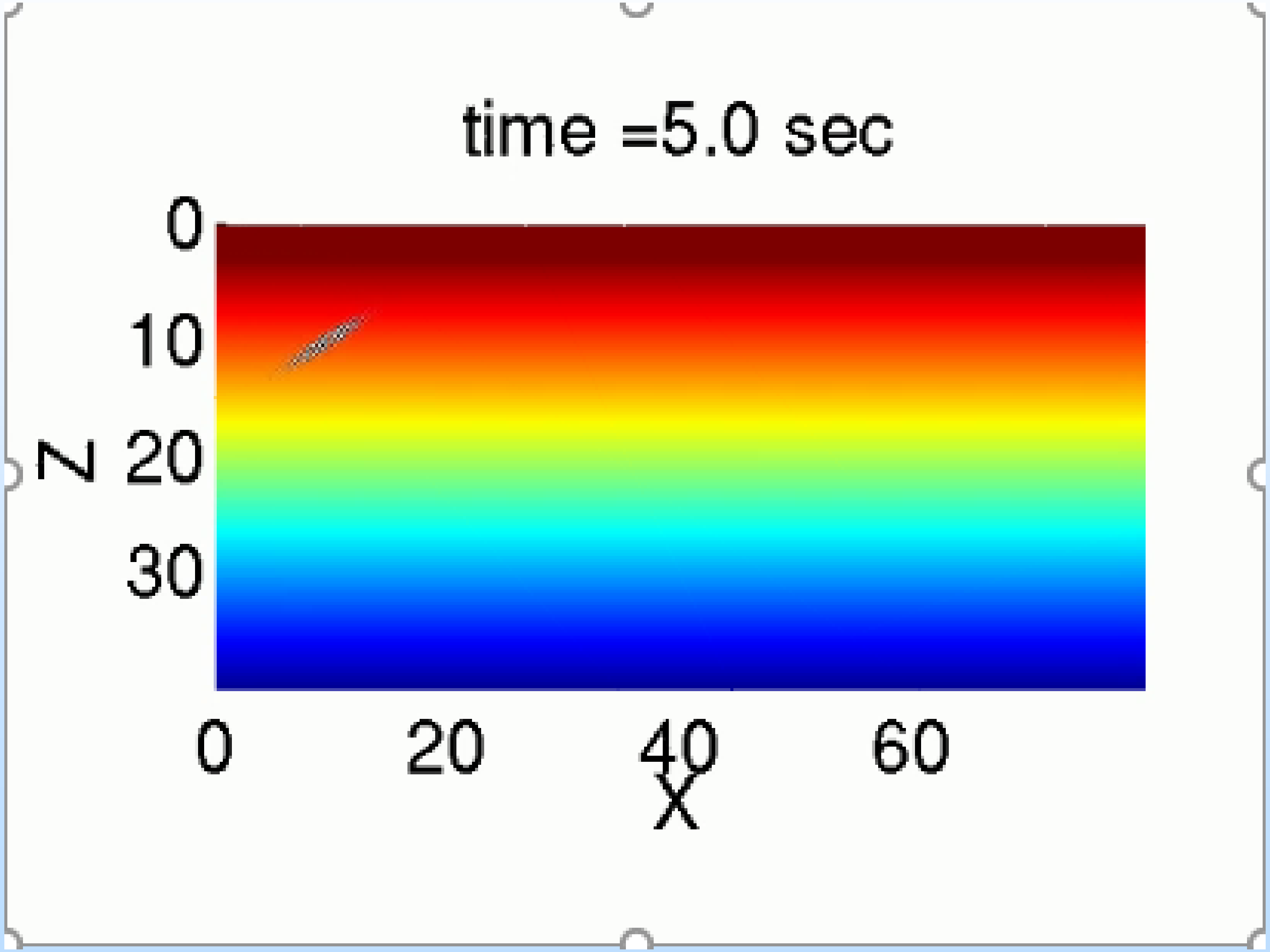

From point sources to localized wave packet

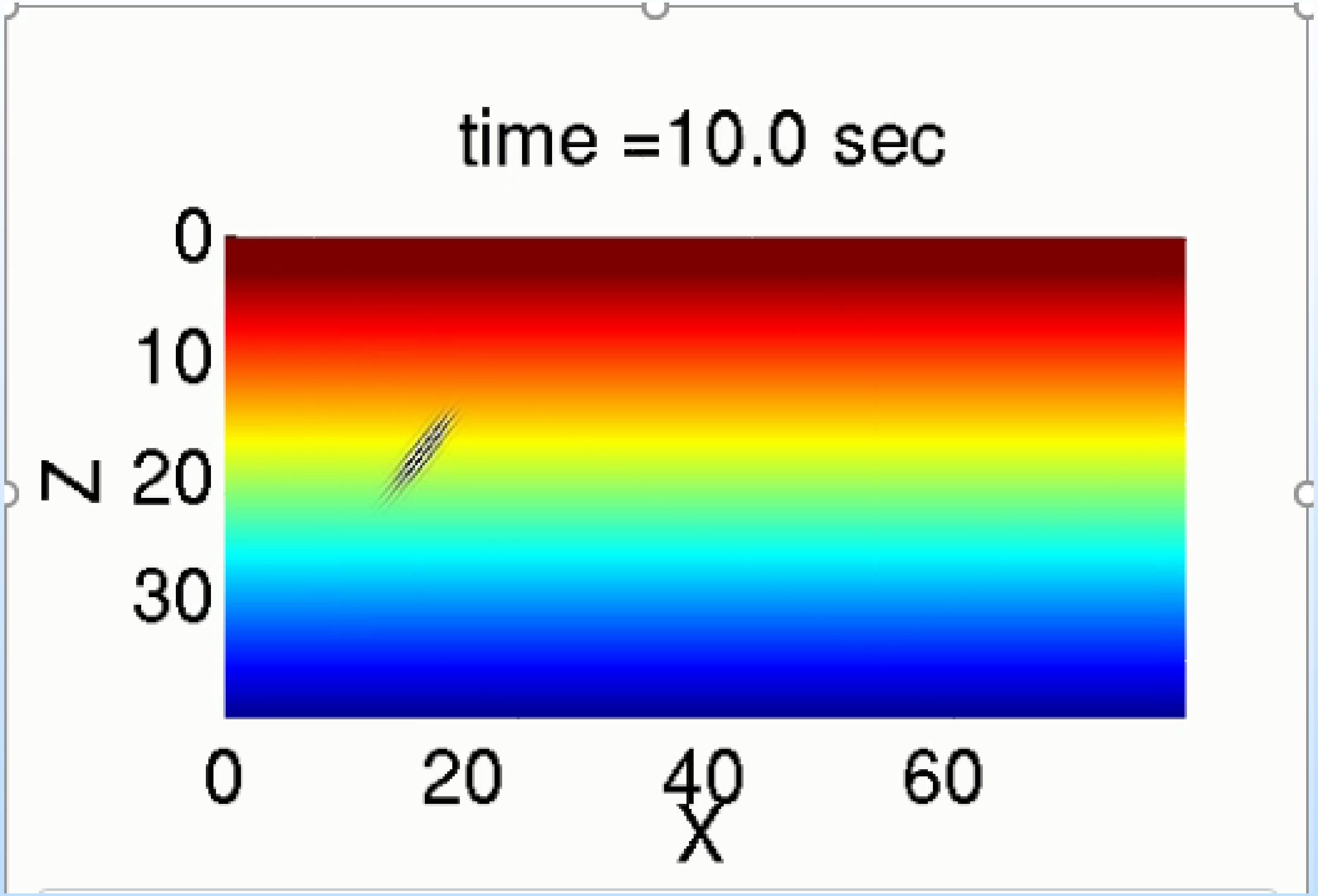

From point sources to localized wave packet

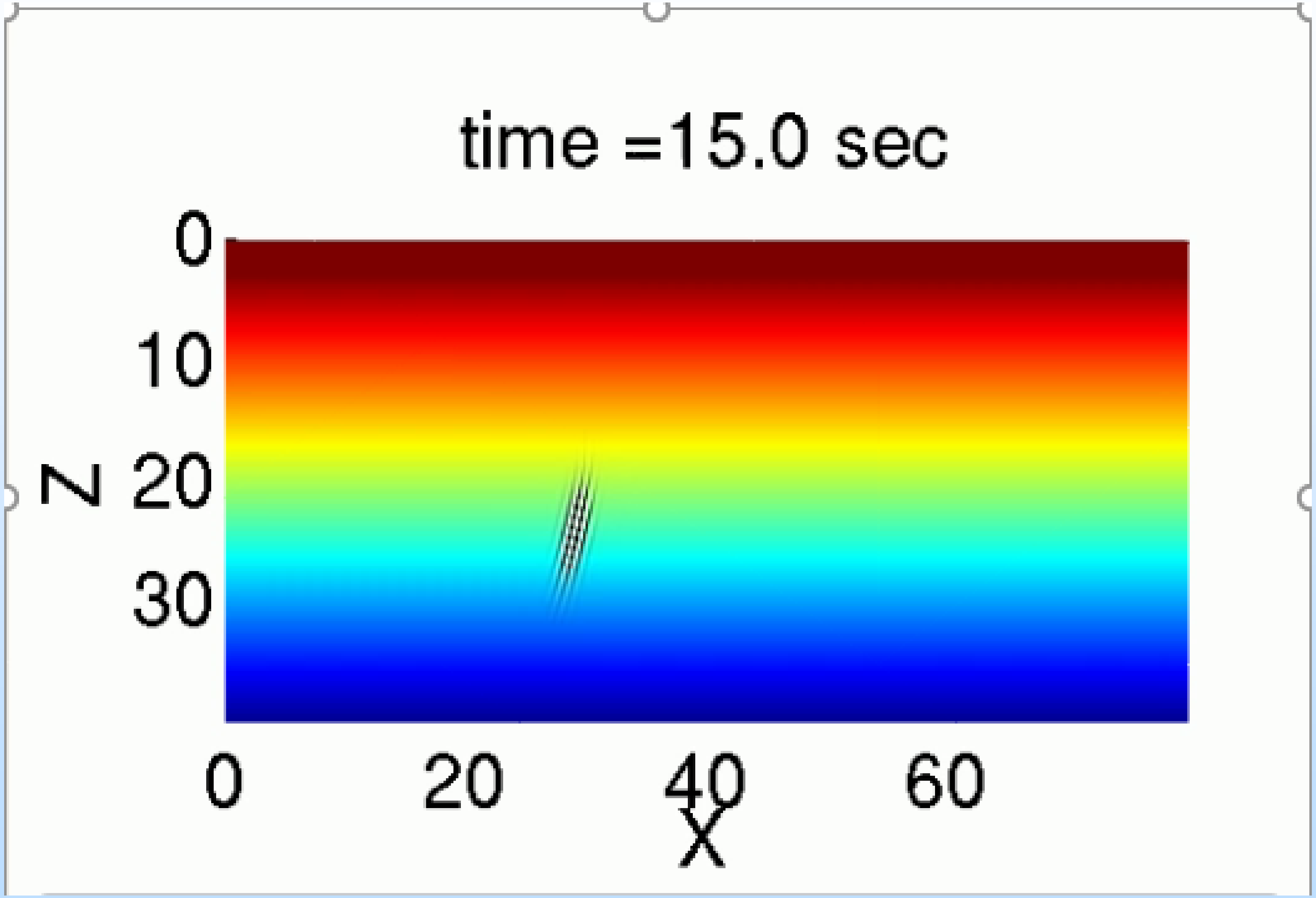

From point sources to localized wave packet

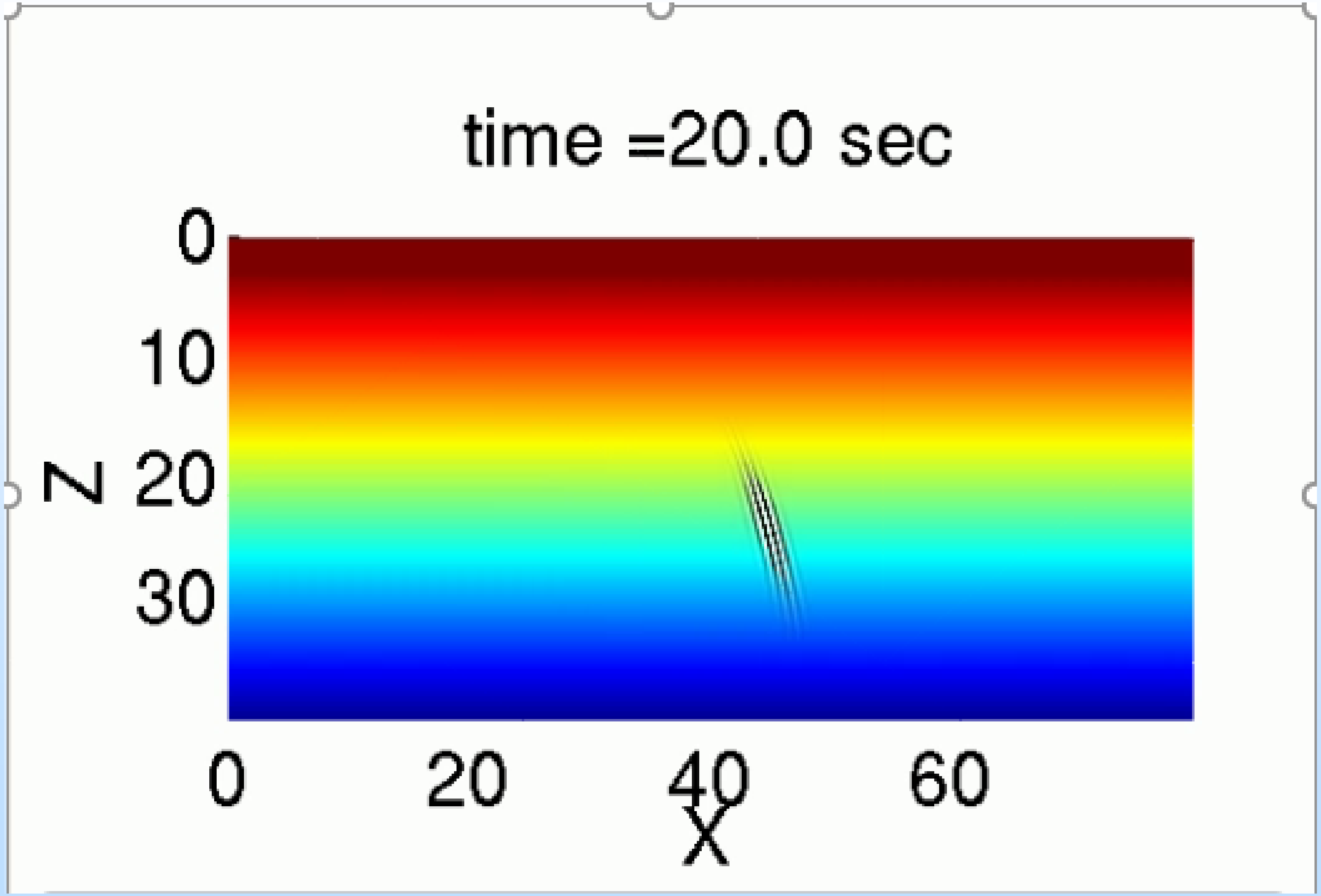

From point sources to localized wave packet

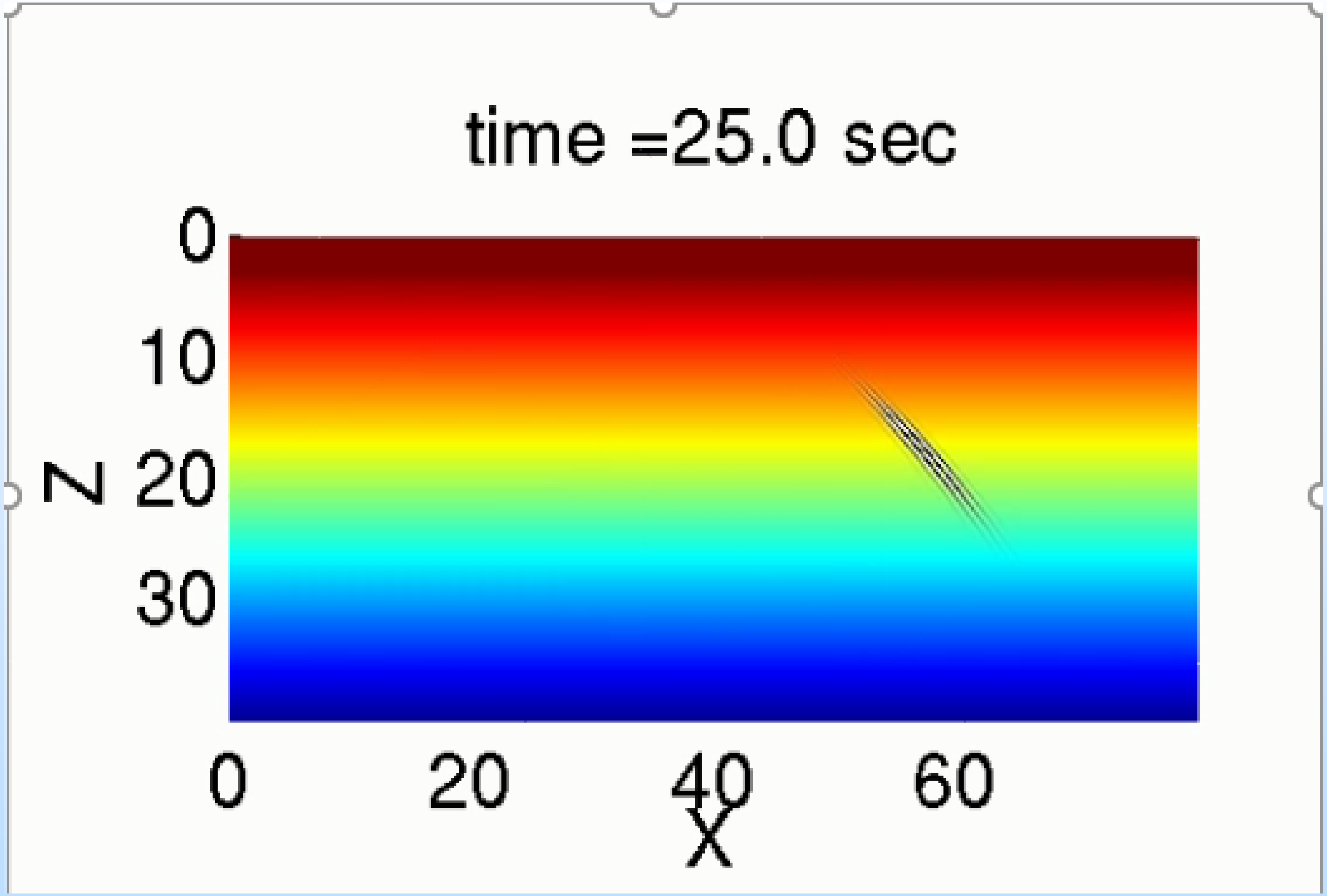

From point sources to localized wave packet

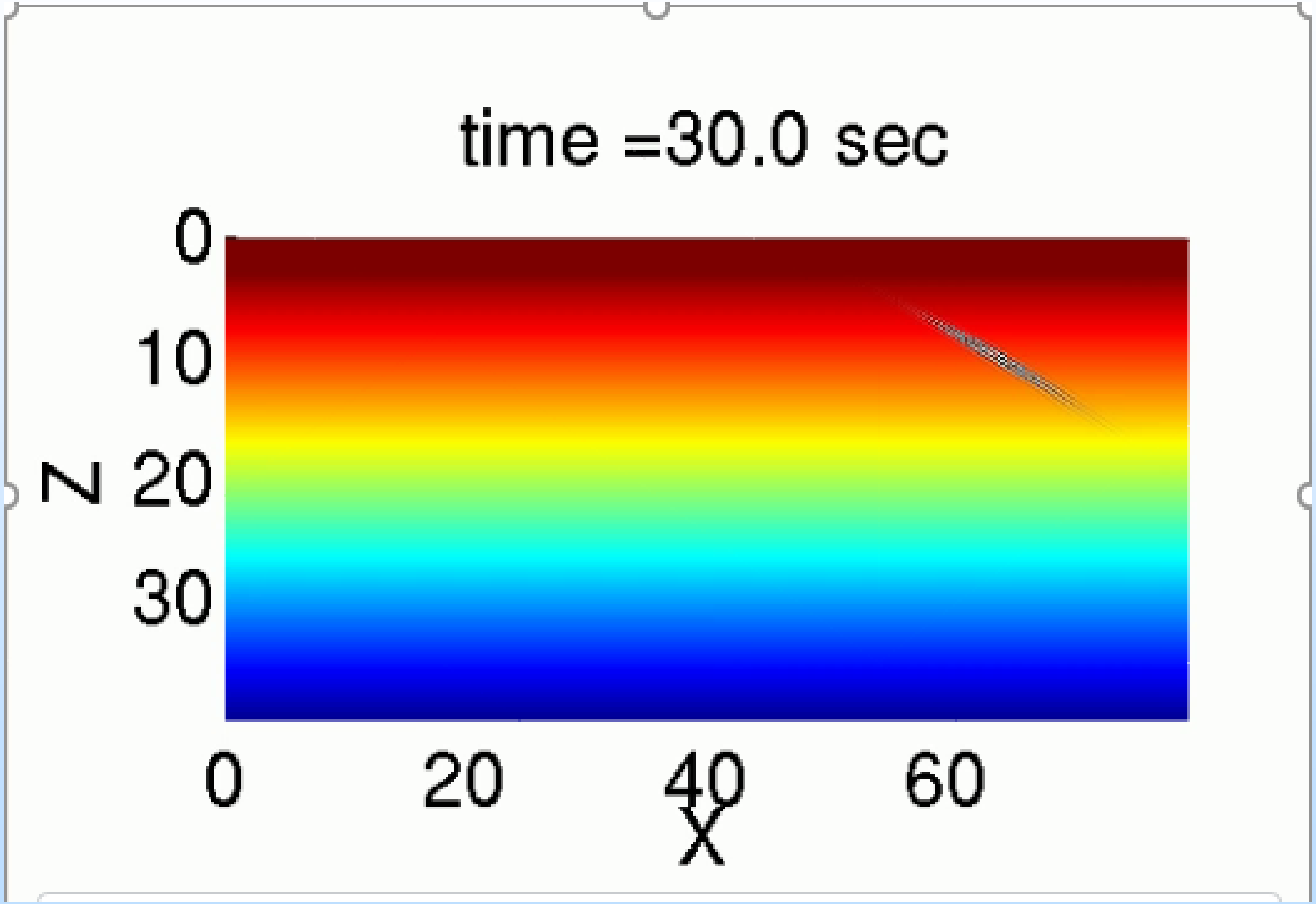

Interference pattern → fractures

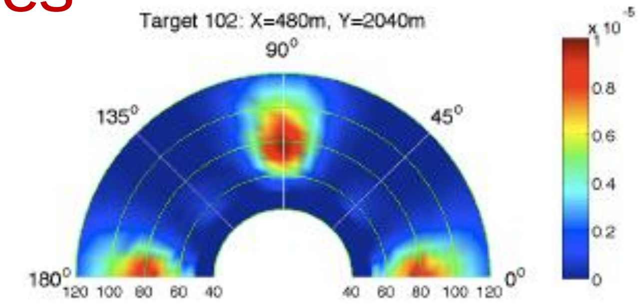

interference pattern
(observation)

Directional wave
incidence

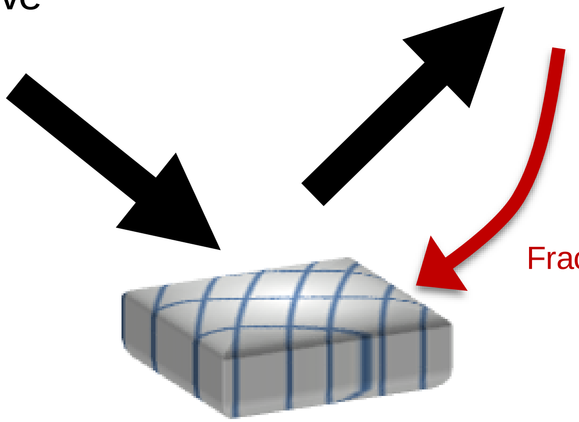

Frac parameter inversion

Fractured reservoir

- Fracture orientation
- Density
- Compliance → fluid permeability (Petrovitch et al., 2013)

Field seismic data (9C) in Montana

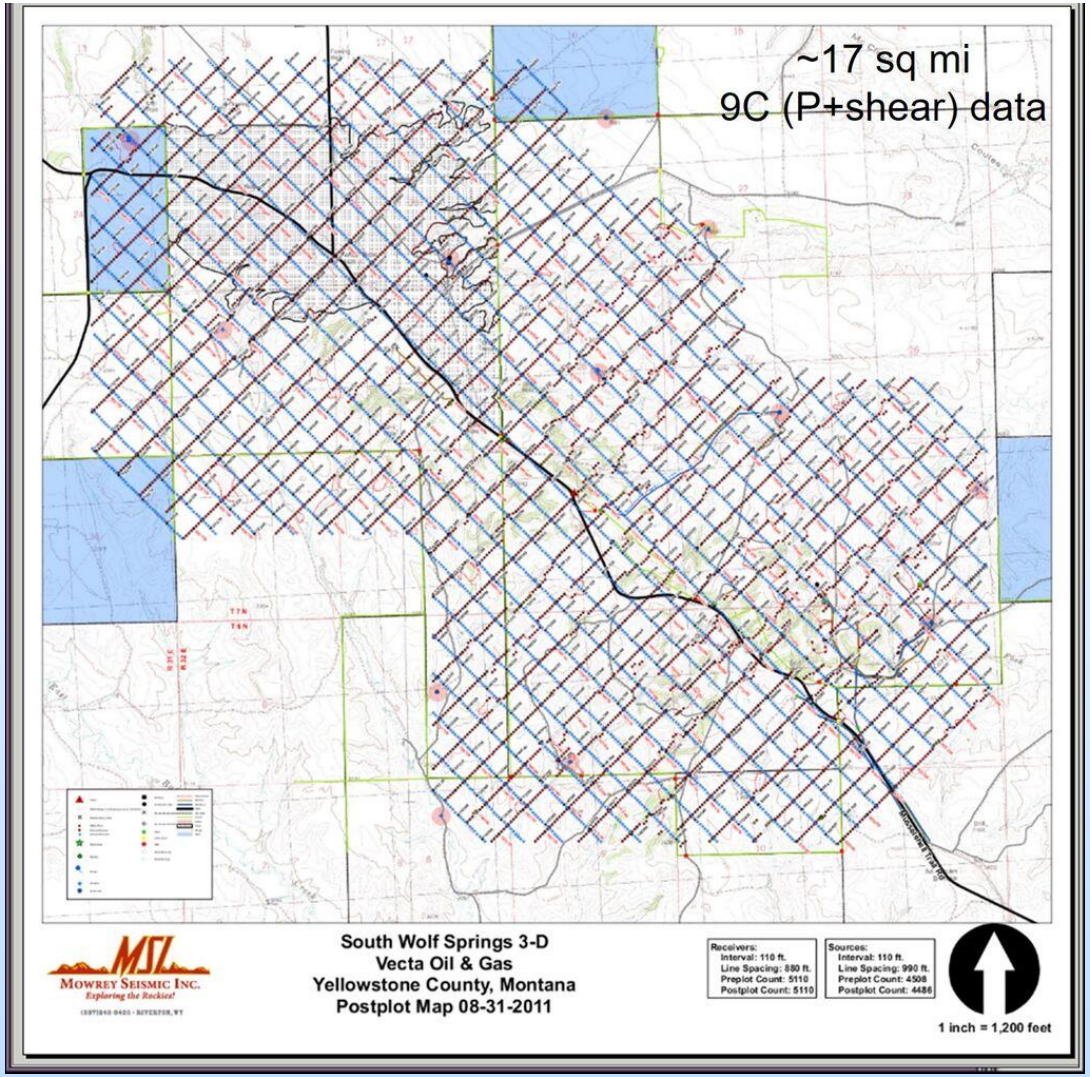

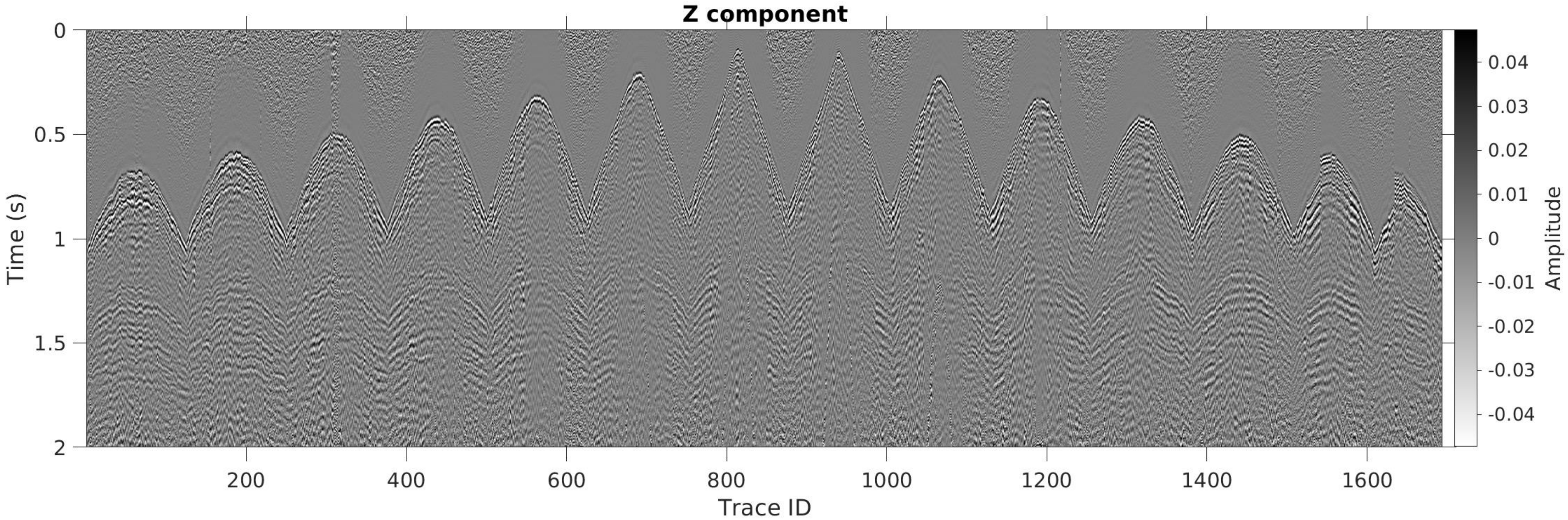

Vertical vibreseis

Fractures and Basement faults

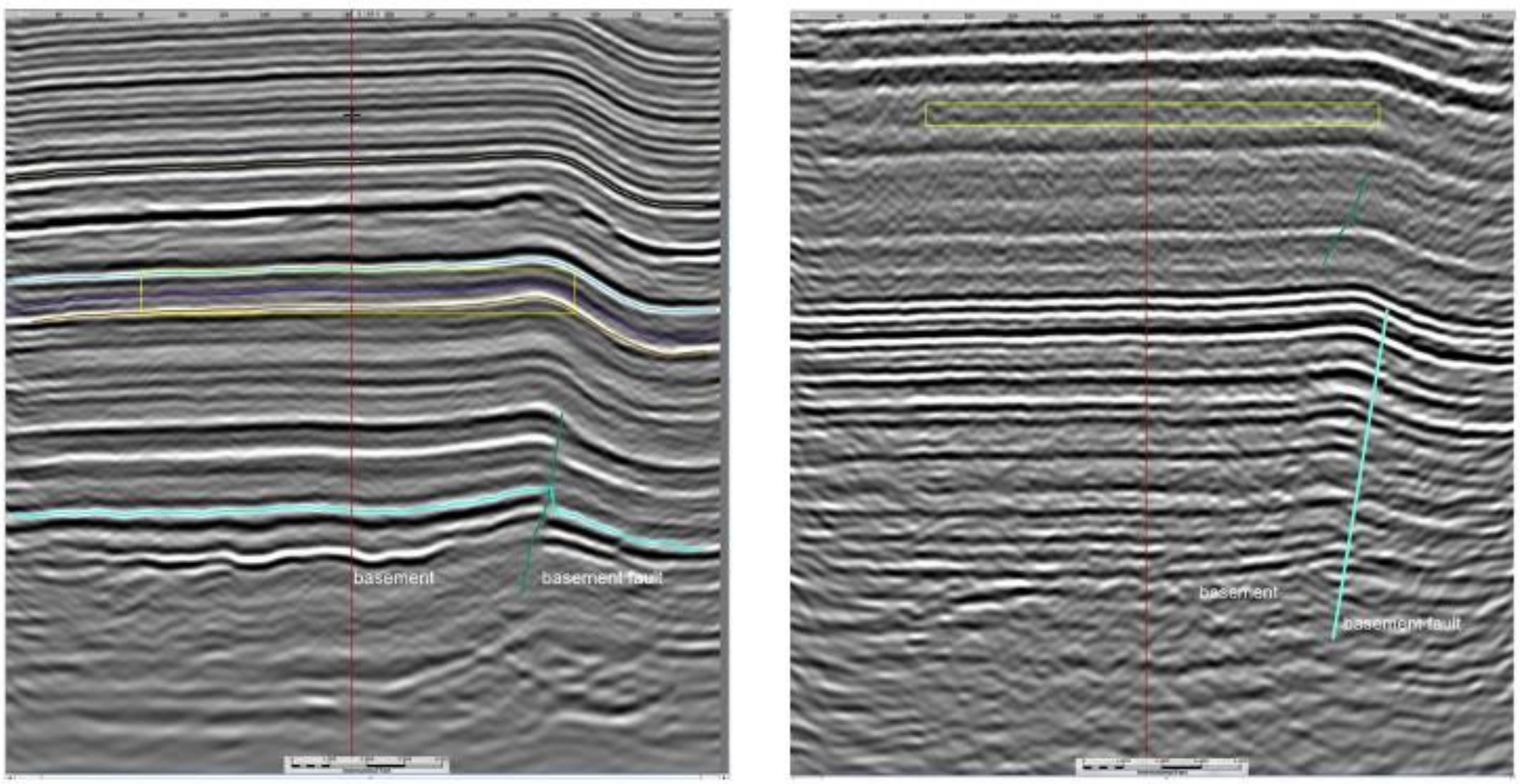

(a) PP image (b) SP image

Build the synthetic elastic model from the field data

P-wave velocity model from the field Vecta data

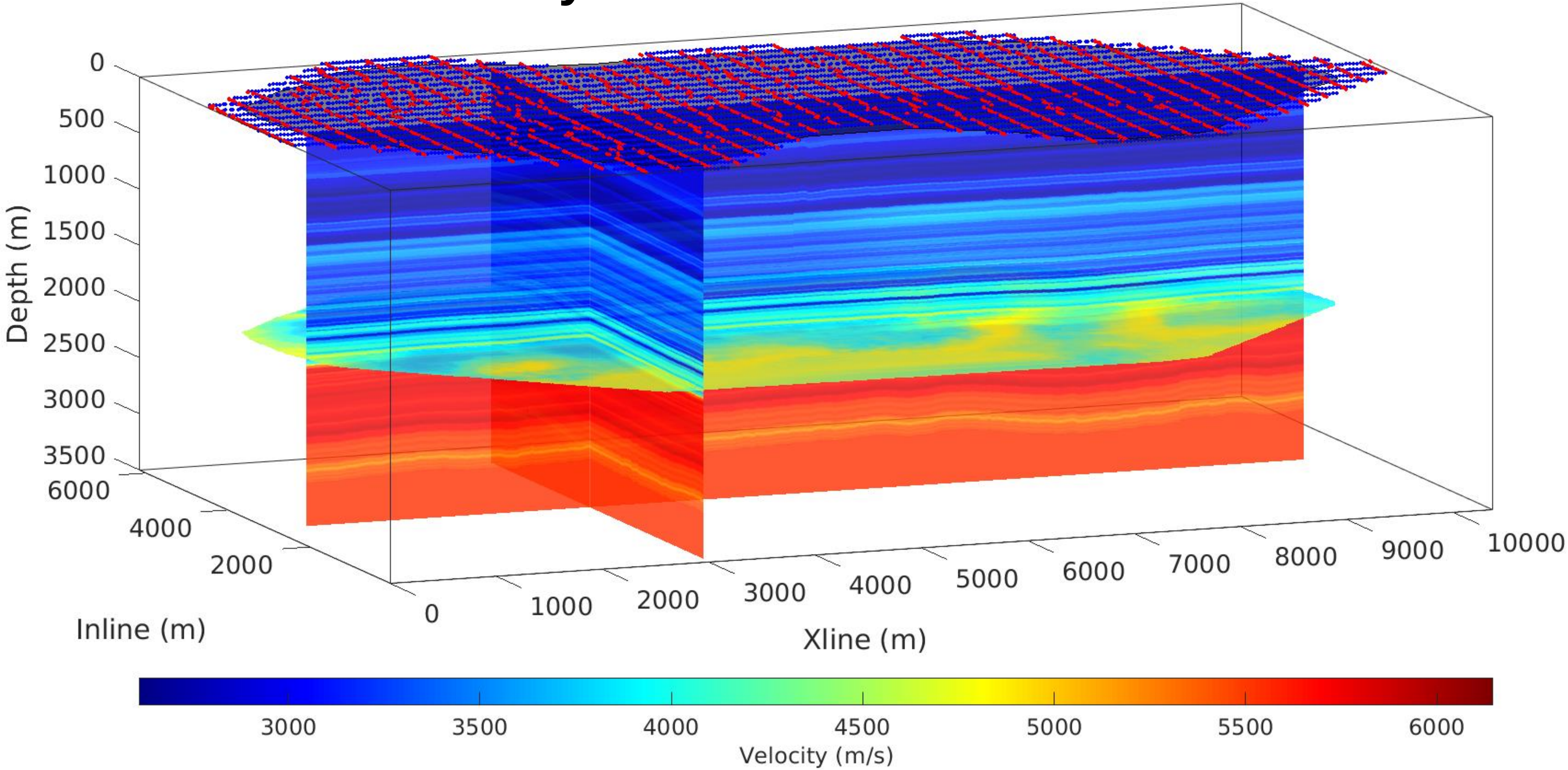

Shear-wave velocity model from the field Vecta data

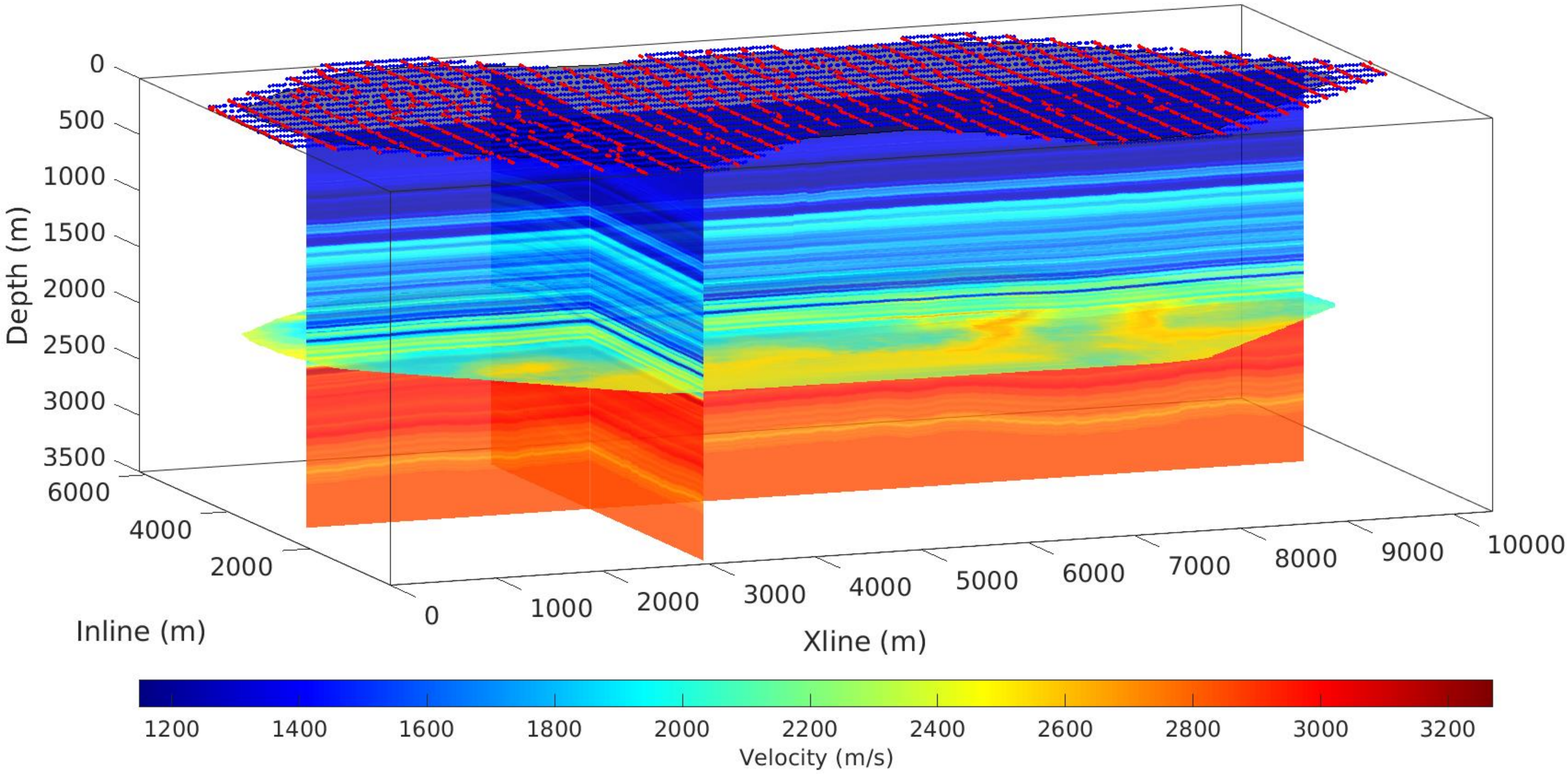

Density model from the field Vecta data

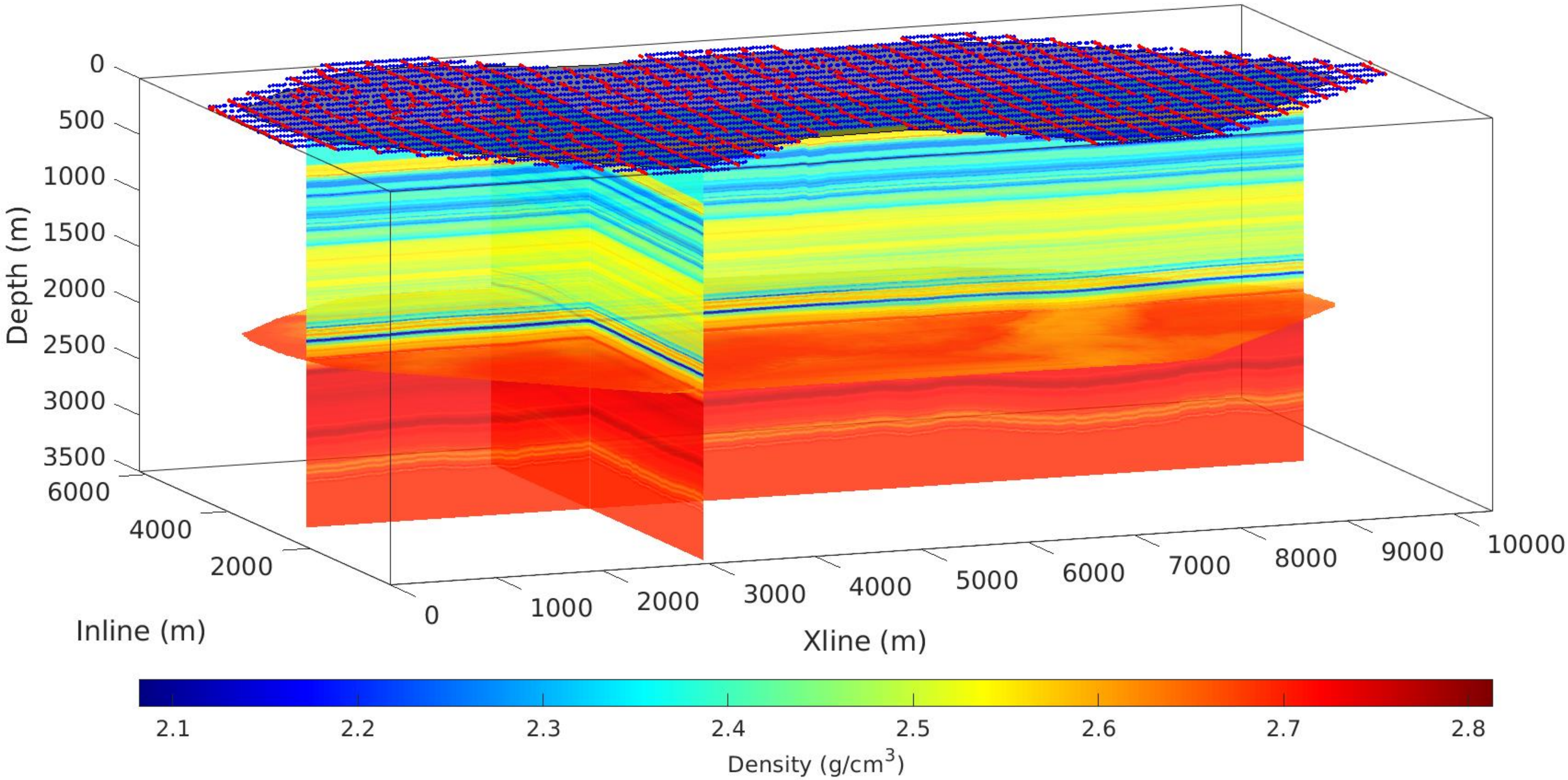

Synthetic Vp model with

: a normal fault

: vertical artificial fracture sets

: small fractures extracted from field data image

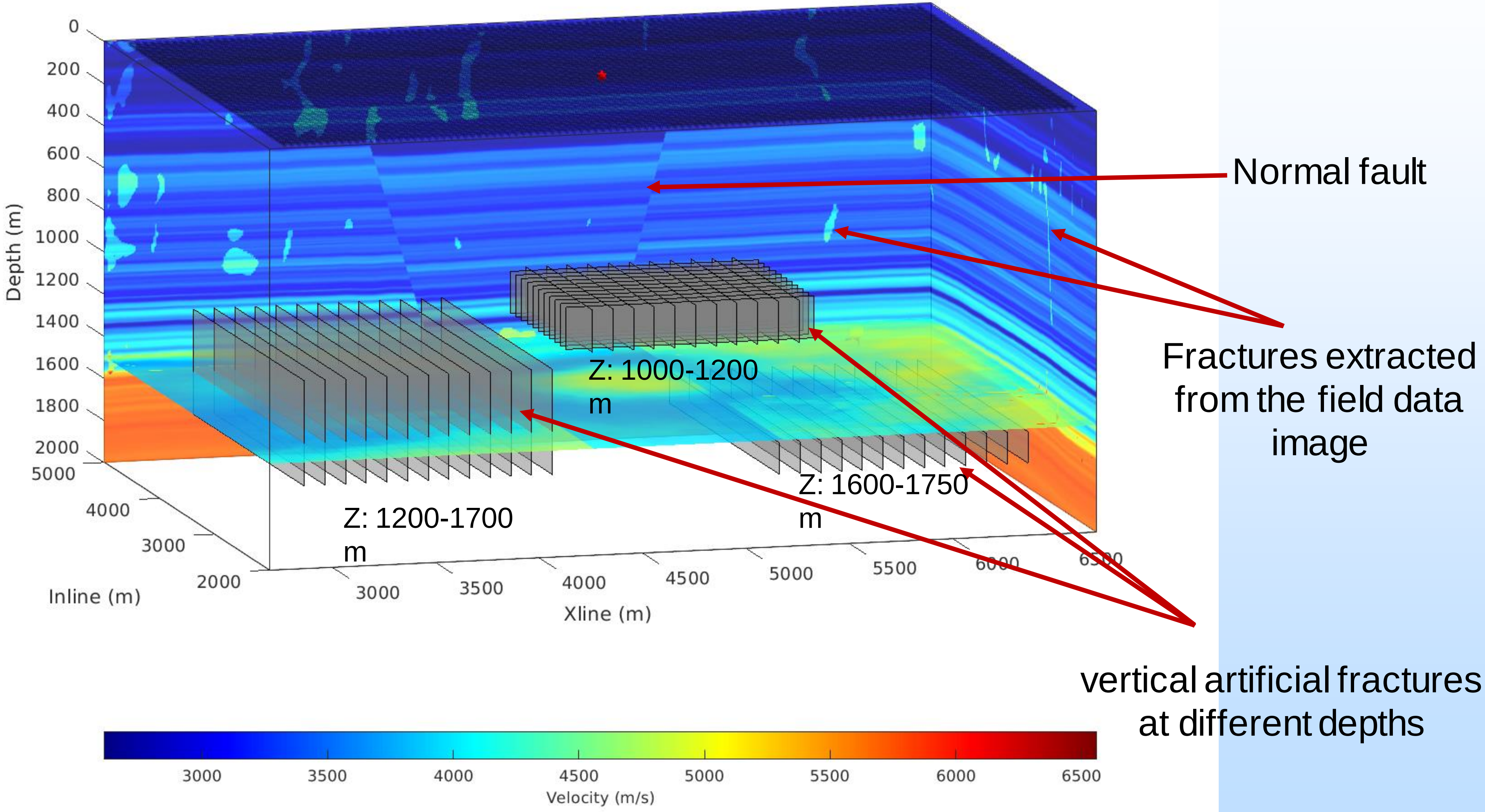

Map view fractures

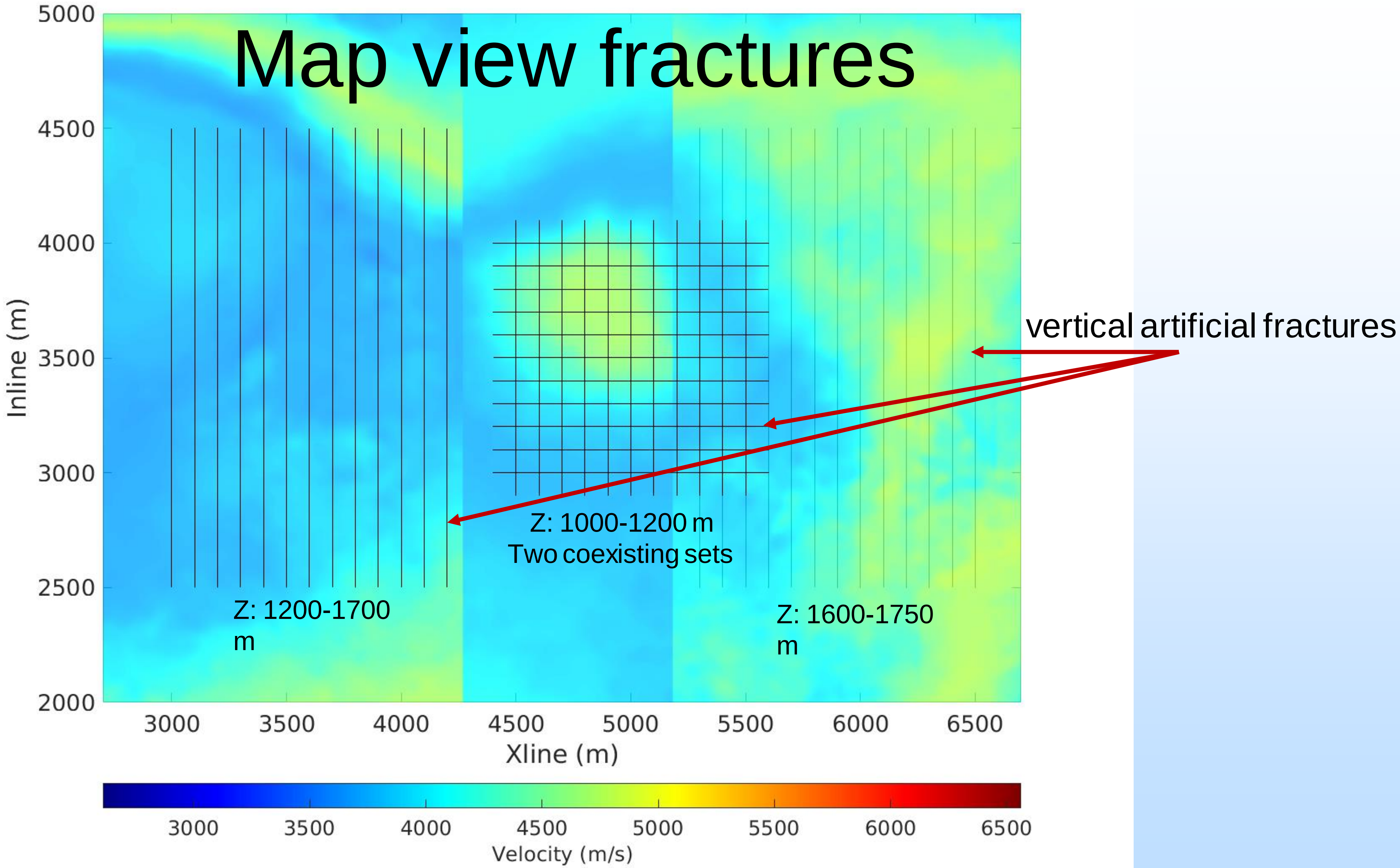

Acquisition geometry

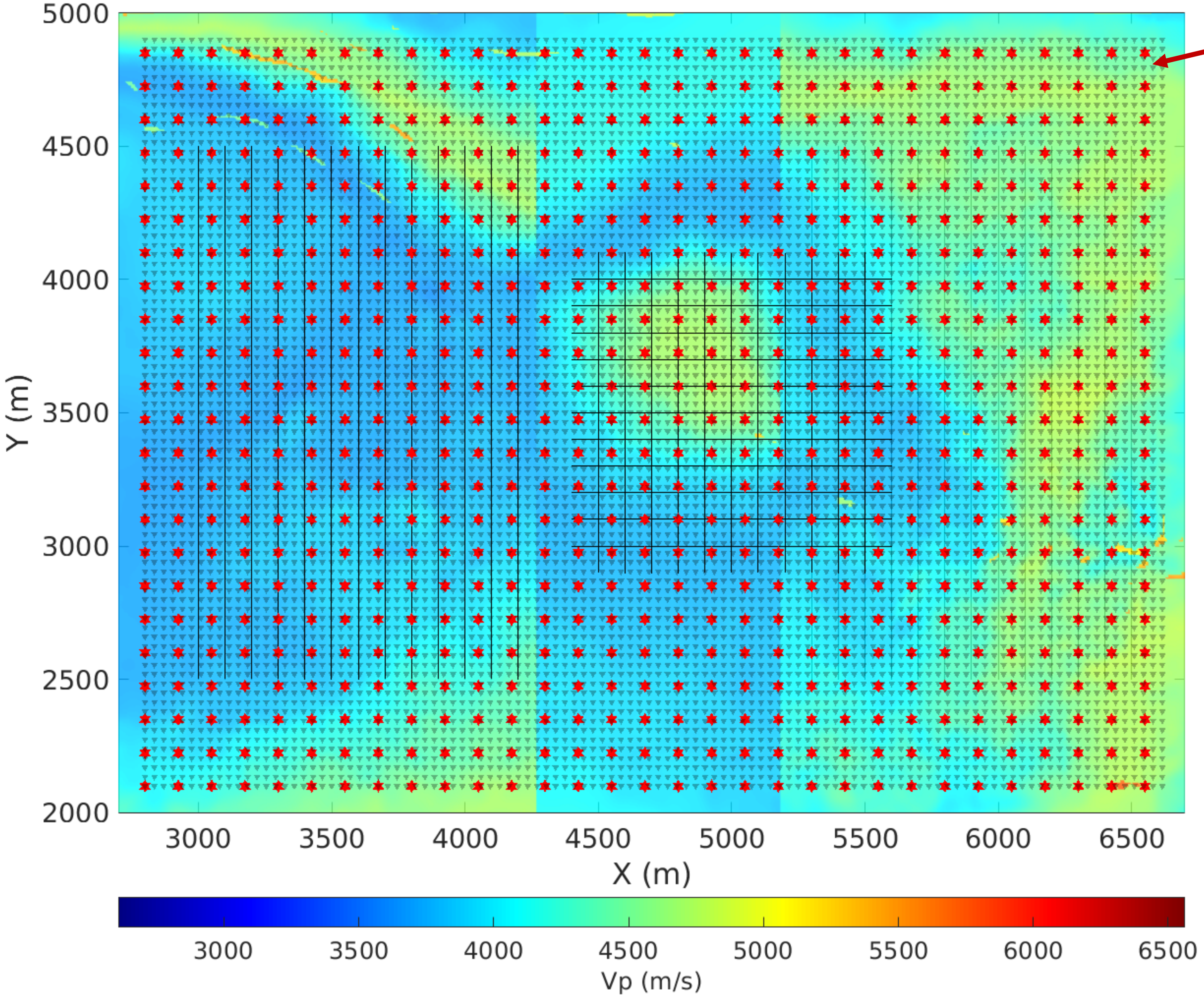

Source
Receiver

Sources:
X: 2800:125:6550 m
Y: 2100:125:4850 m
Total: 31*23=**713**

Receivers:
X: 2800:35:6615 m
Y: 2100:35:4900 m
Total: 110*81=**8910**

Both Source and receivers are at surface

Modeled common-shot gathers at one location with different types of source.

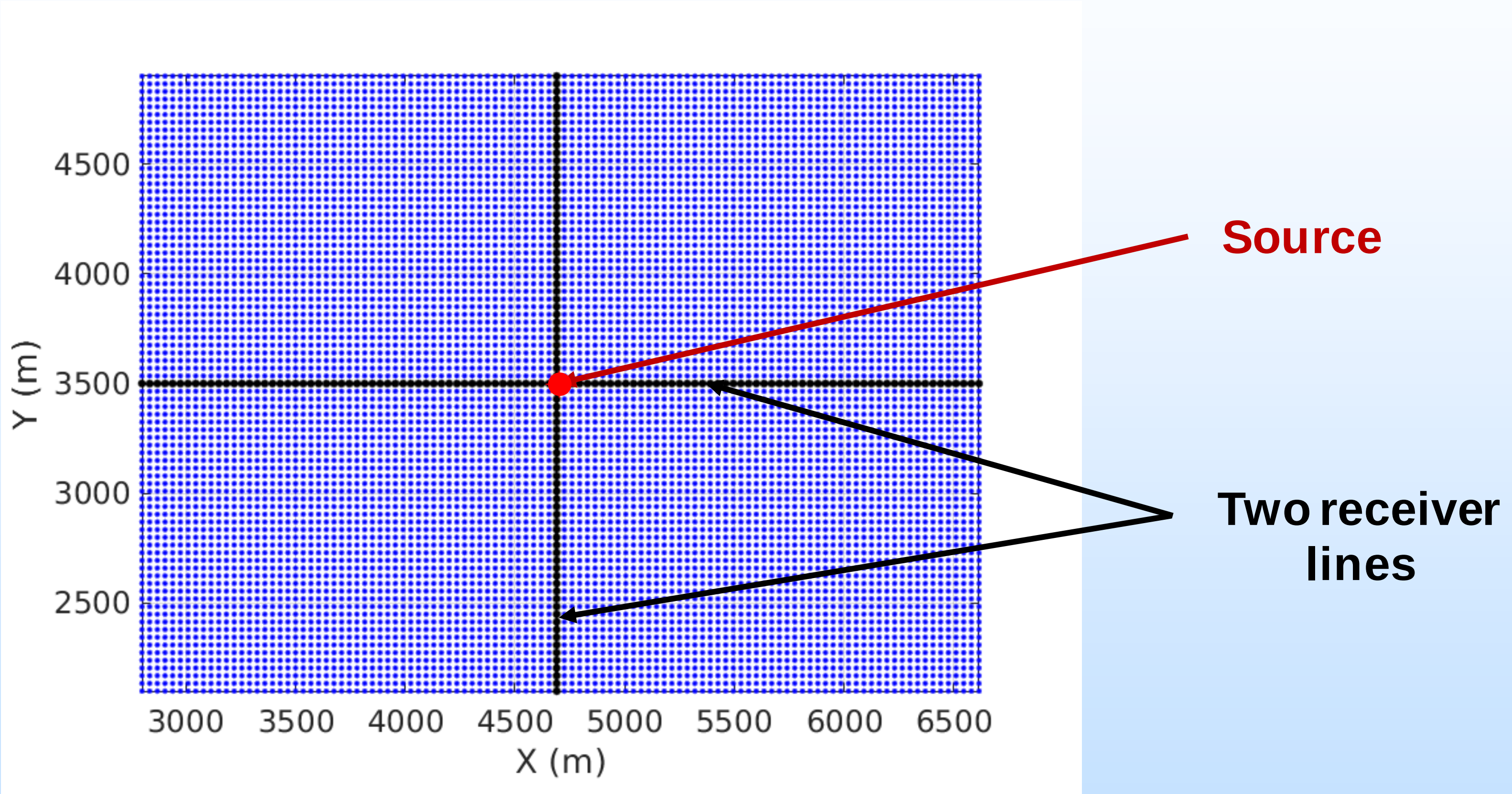

Source wavelet: 20 Hz Ricker

Receivers along X

Receivers along Y

Explosive source

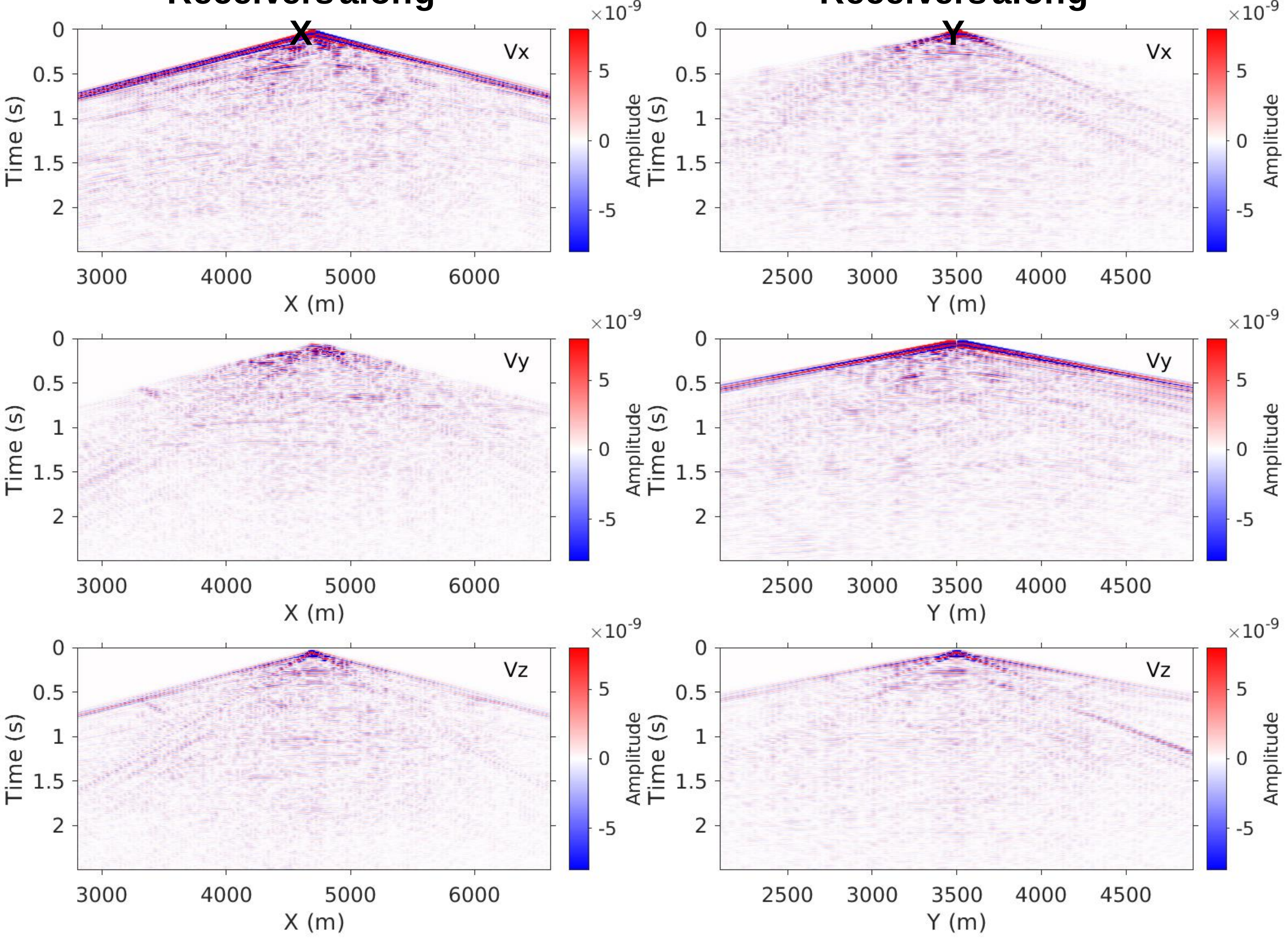

Single force: X

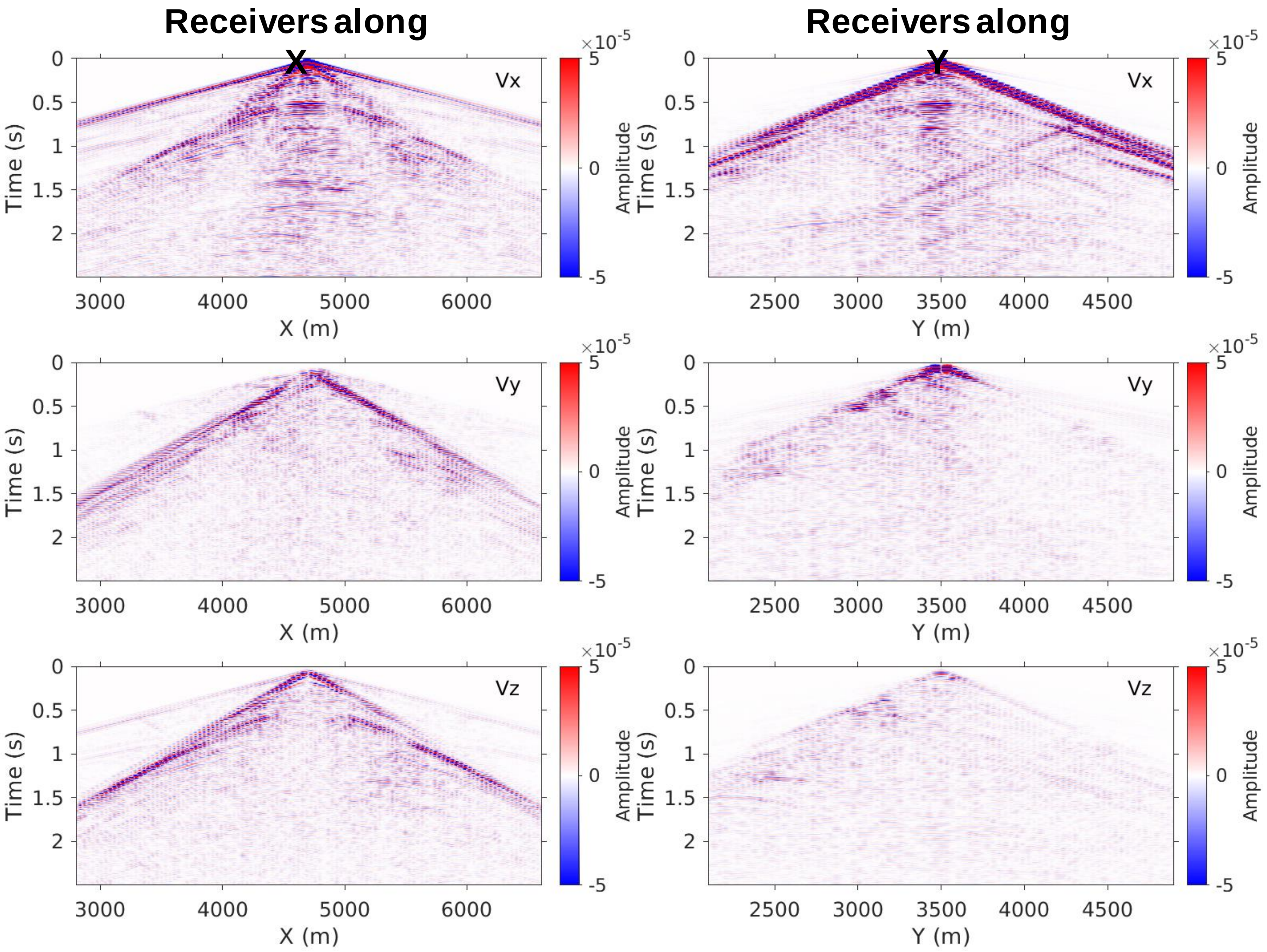

Receivers along X

Receivers along Y

Single force: Y

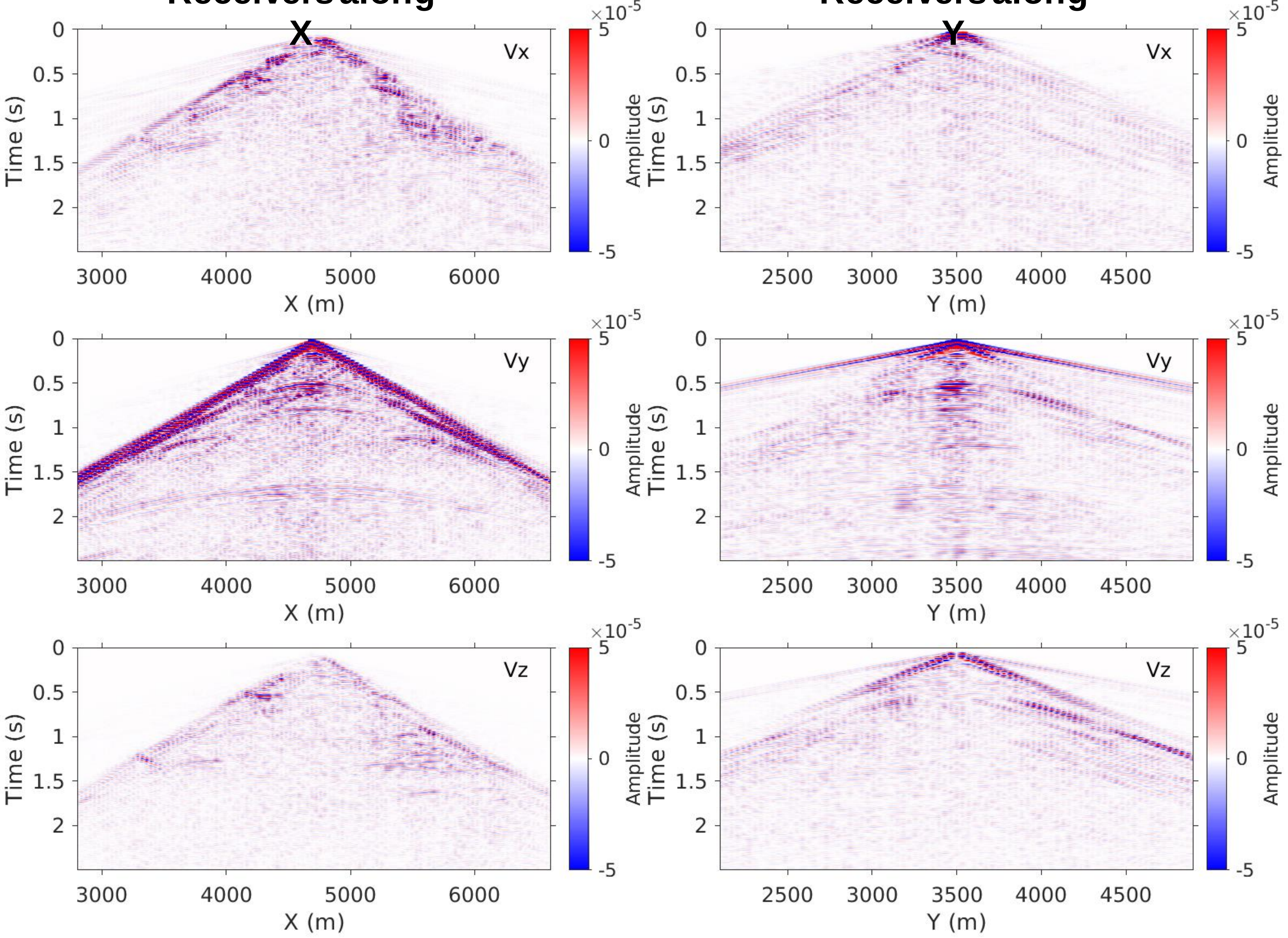

Single force: Z

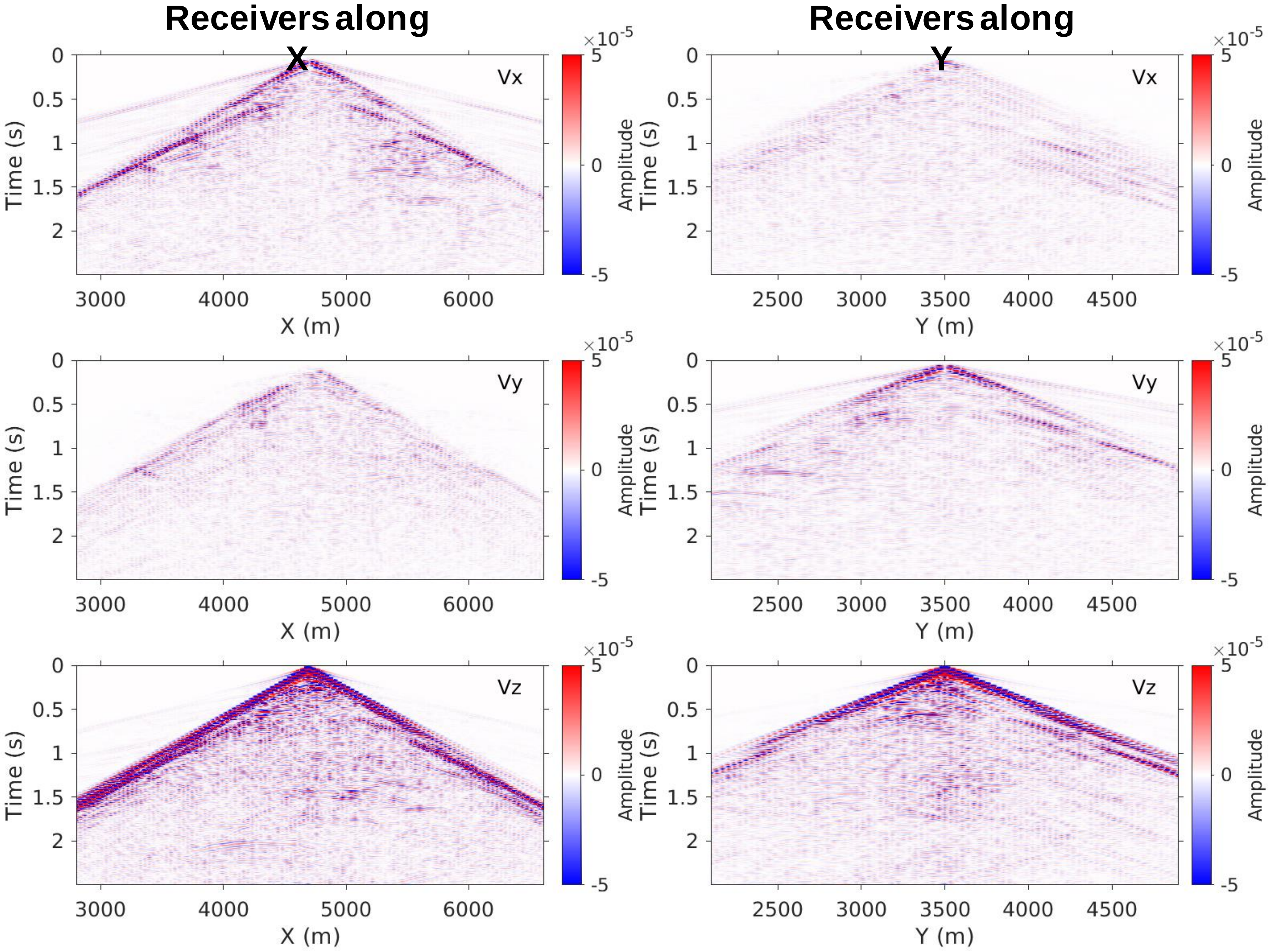

Fracture detection results using The Seismic Double-Beam method

Top view of detected fractures

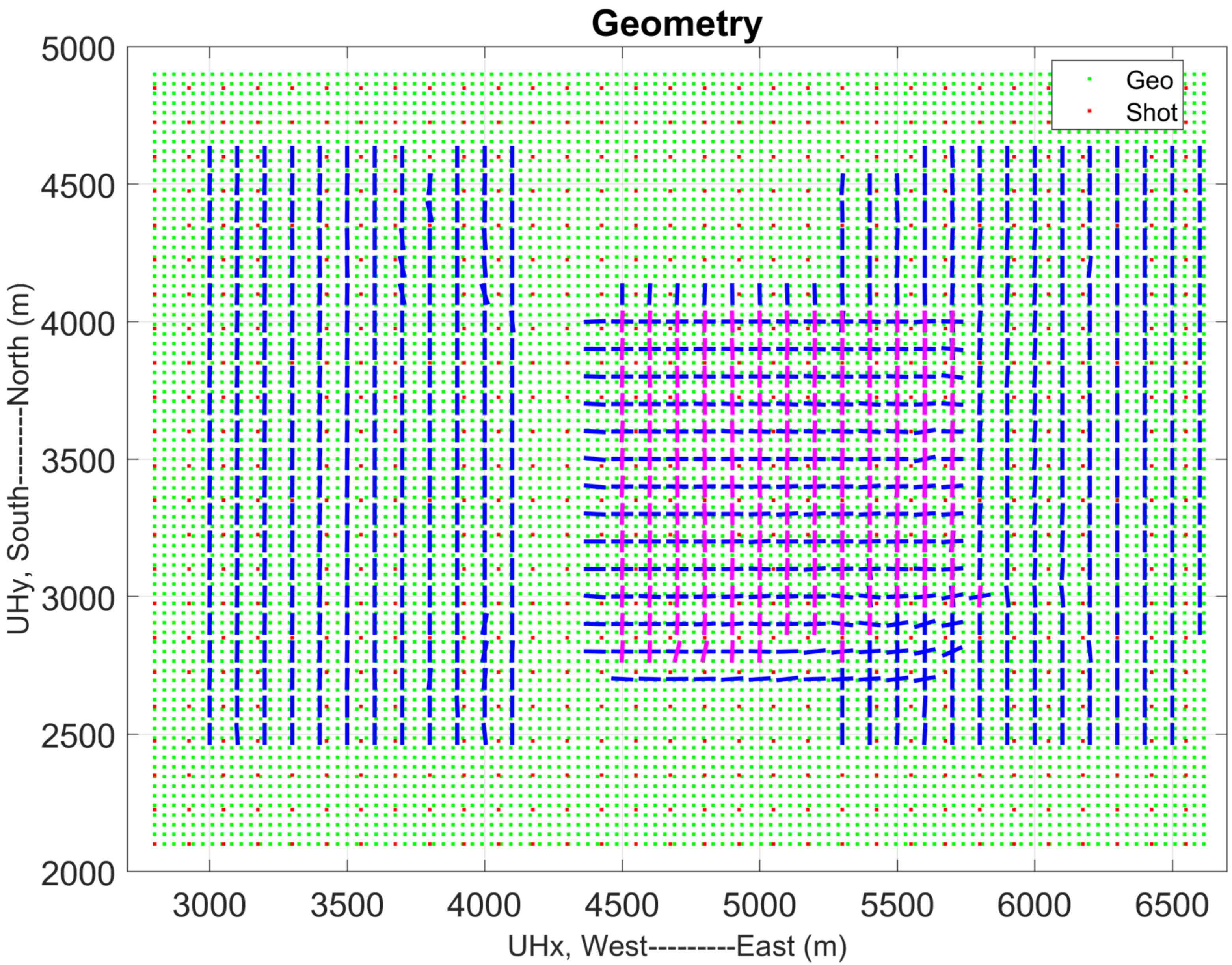

At three depths (1100 m, 1400 m and 1650 m) from frequencies 15 Hz, 20 Hz, 30 Hz and 40 Hz

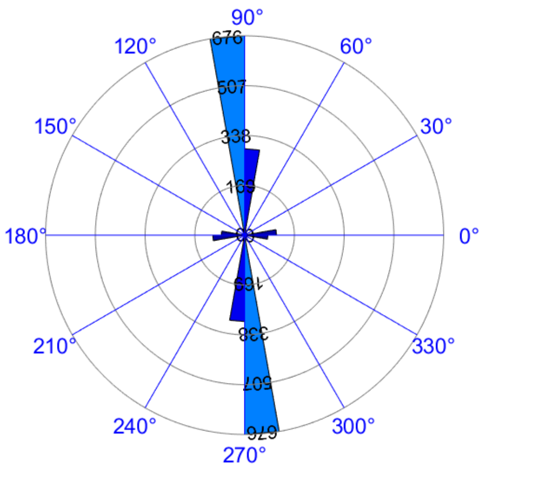

3D view of detected fractures

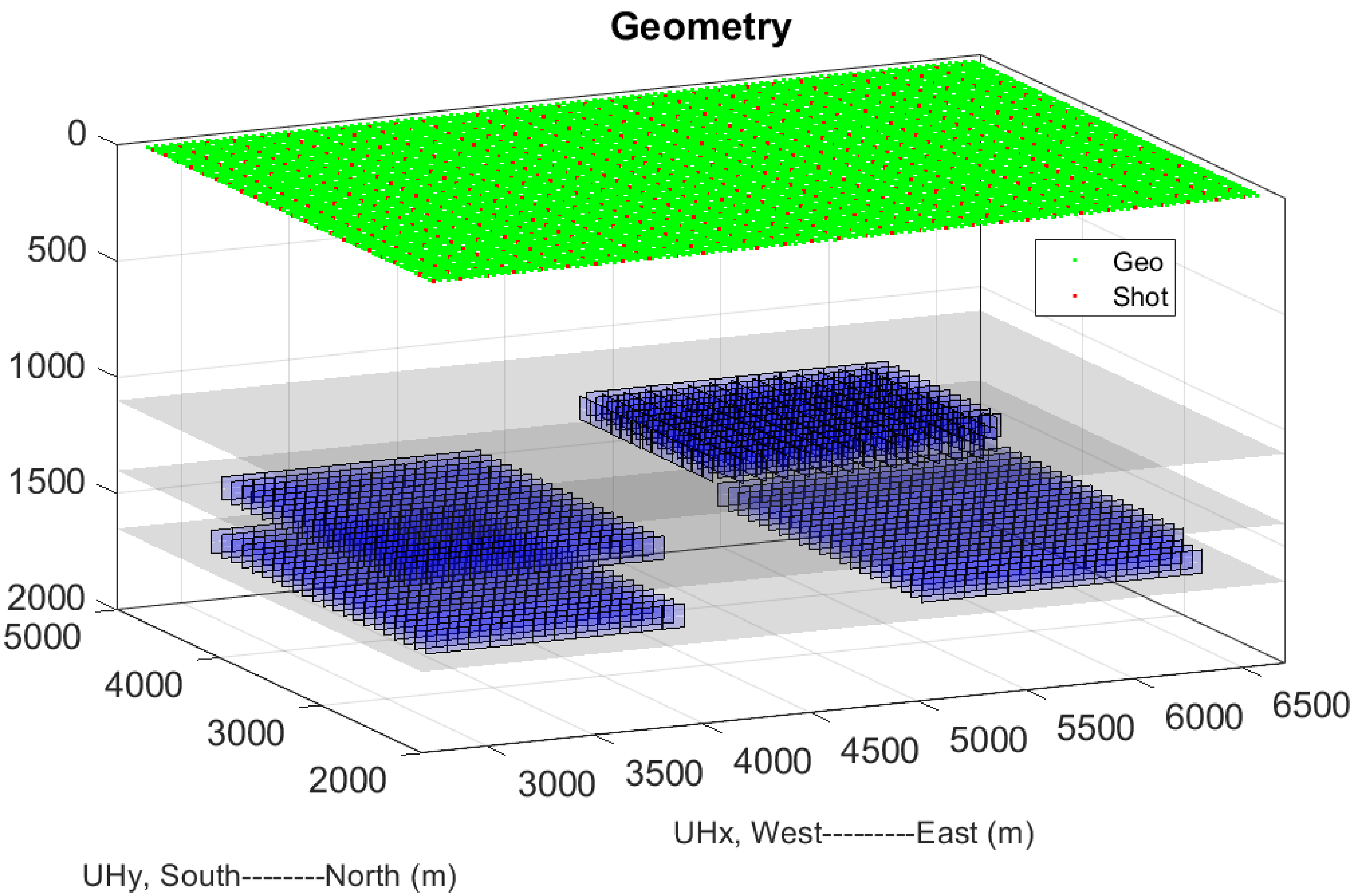

Example of DB images

Depth 1100 m: **Has** fractures

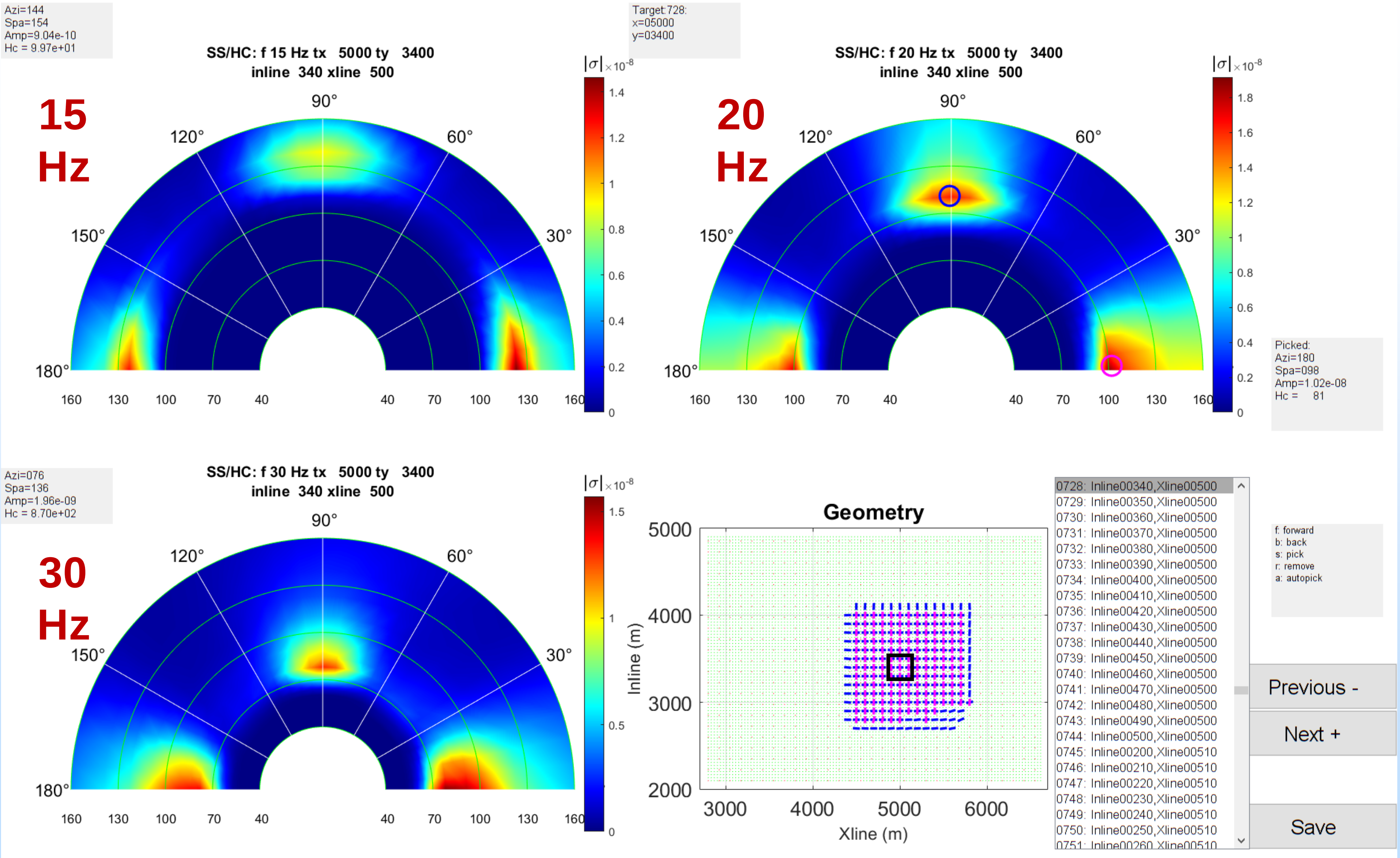

Depth 1400 m: **Has** fractures

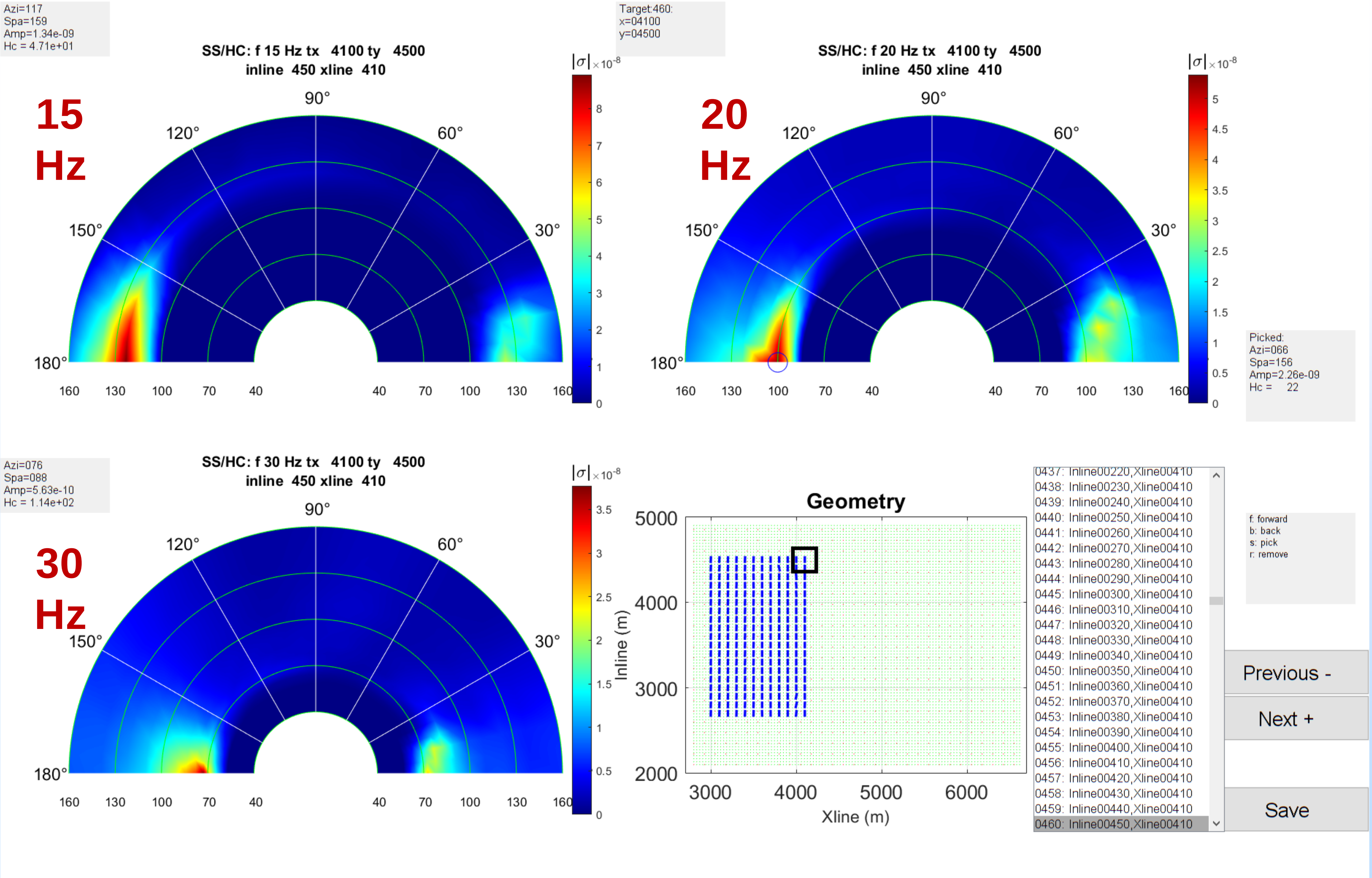

Depth 1400 m: **Has** fractures

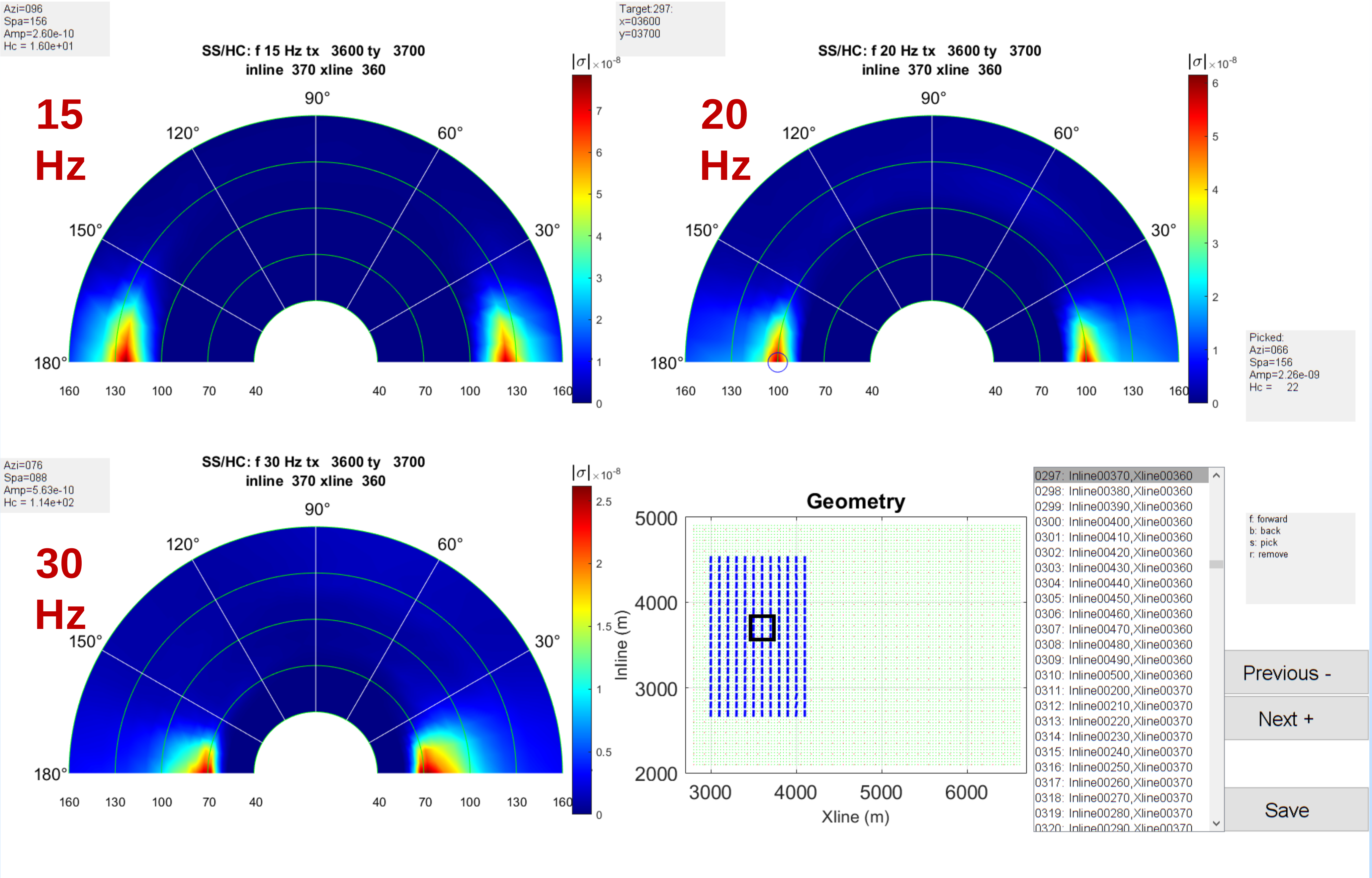

Depth 1650 m: Has fractures

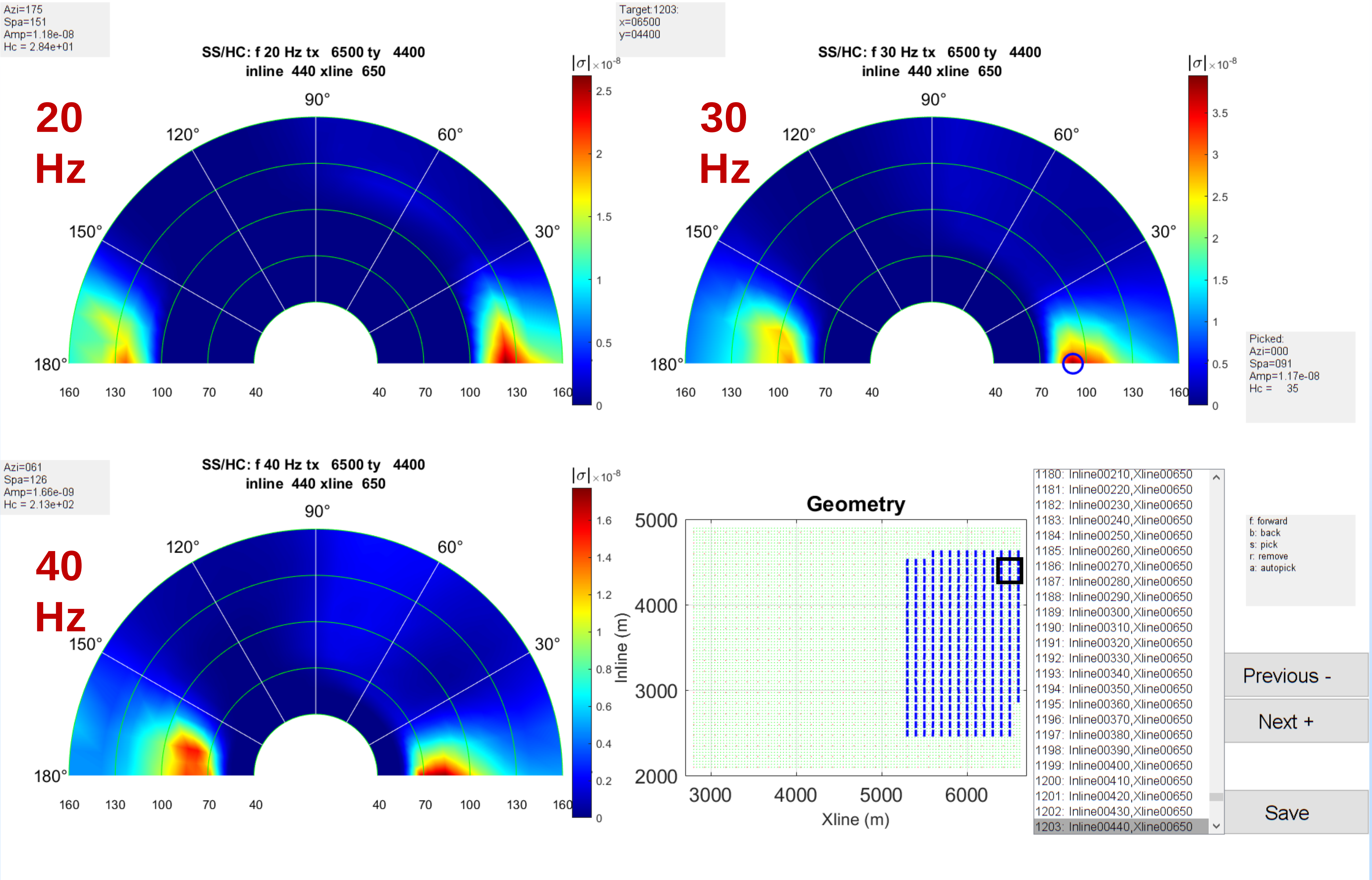

Depth 1100 m: No fracture

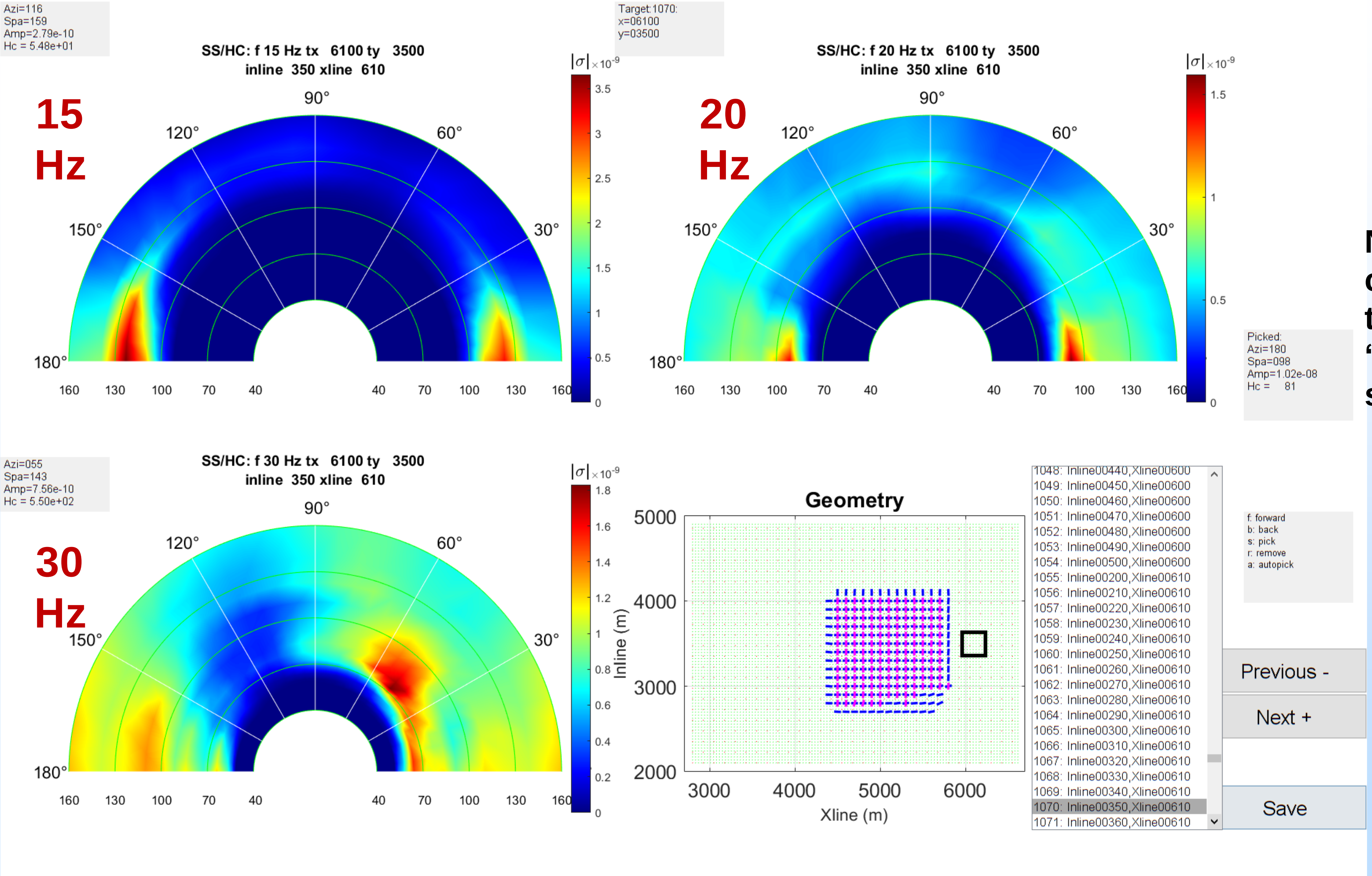

No consistent focused "bright spot"

Depth 1400 m: No fracture

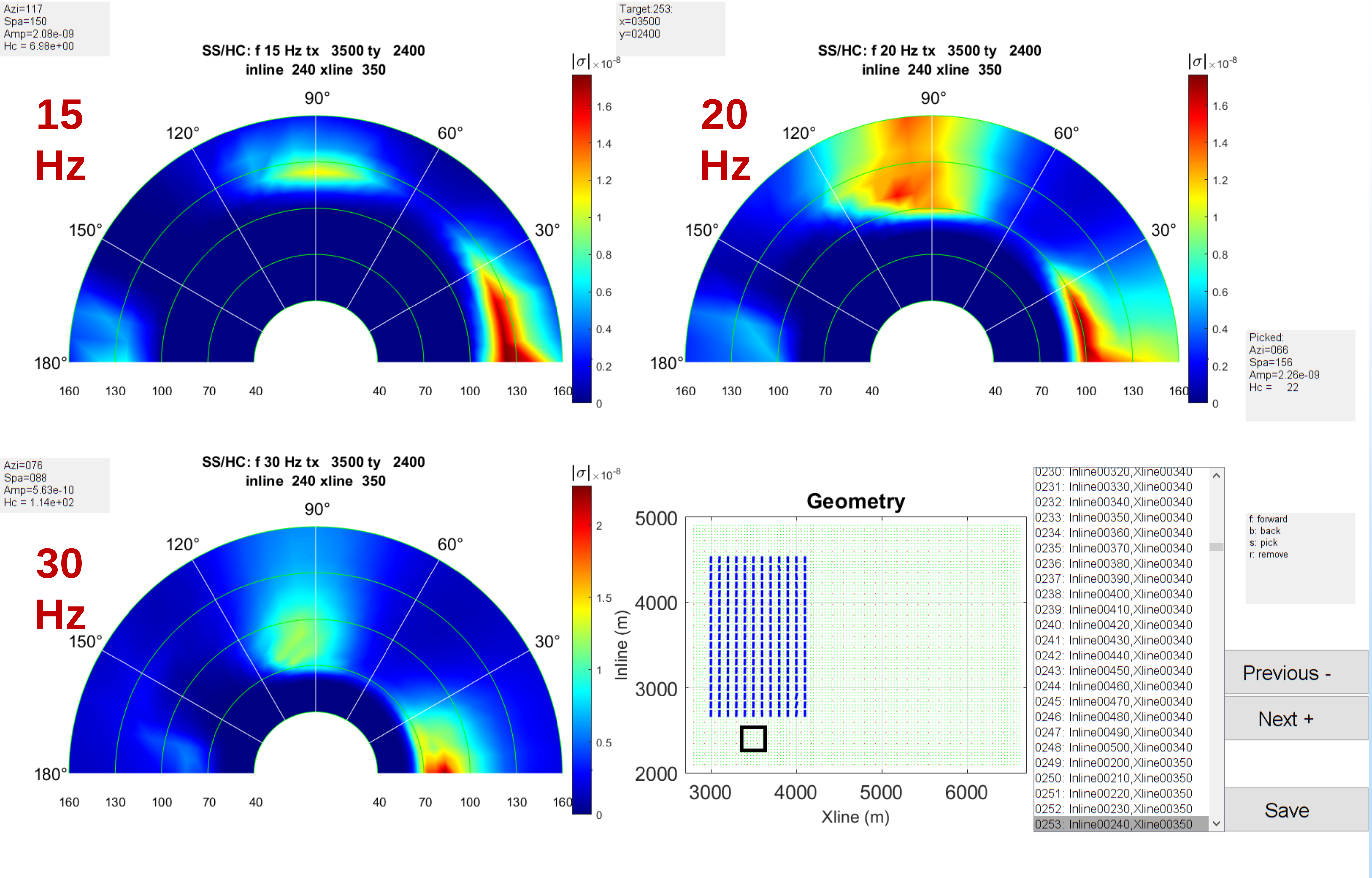

Depth 1400 m: No fracture

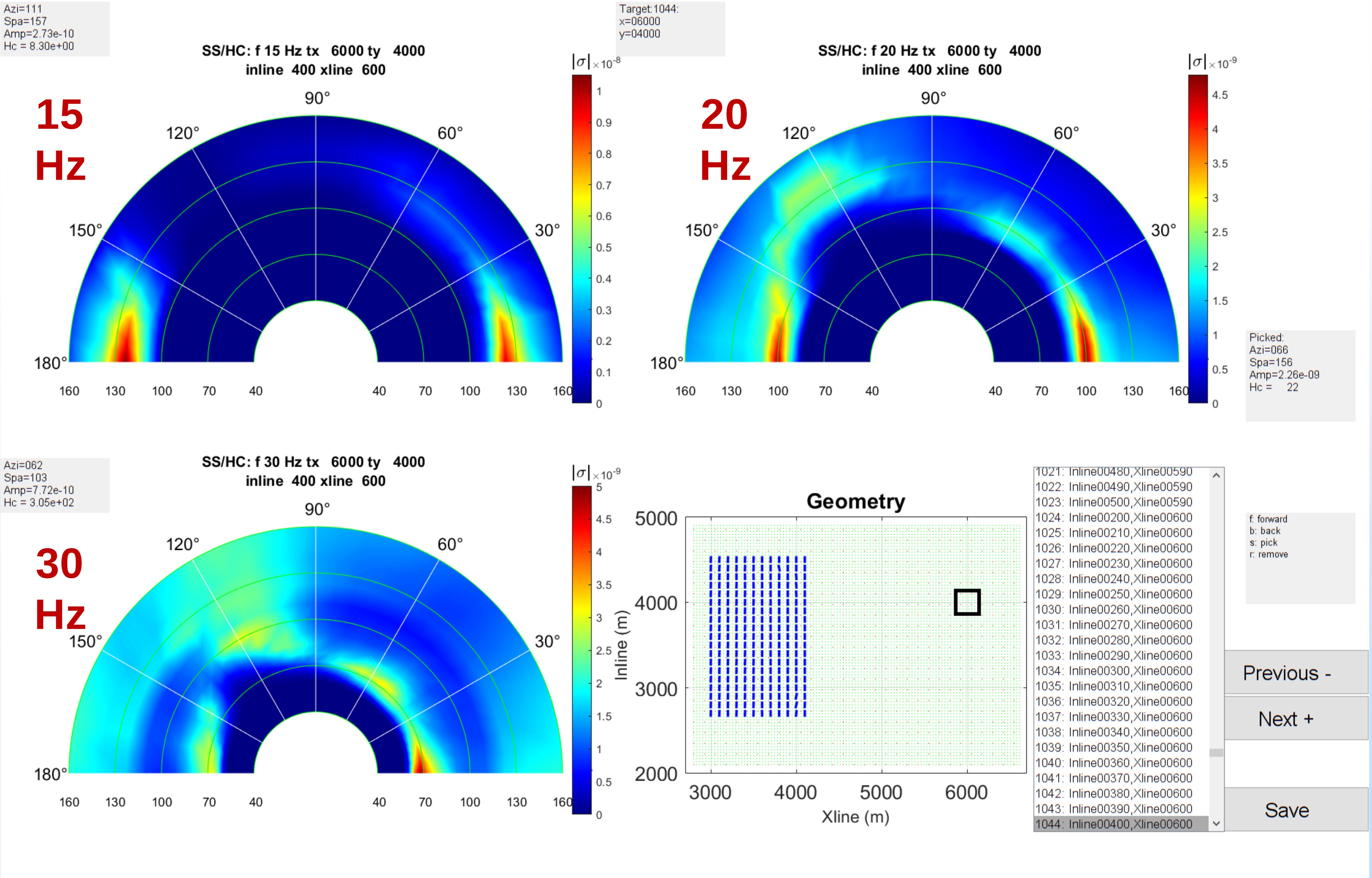

Next steps: discrete fracture network using Machine learning

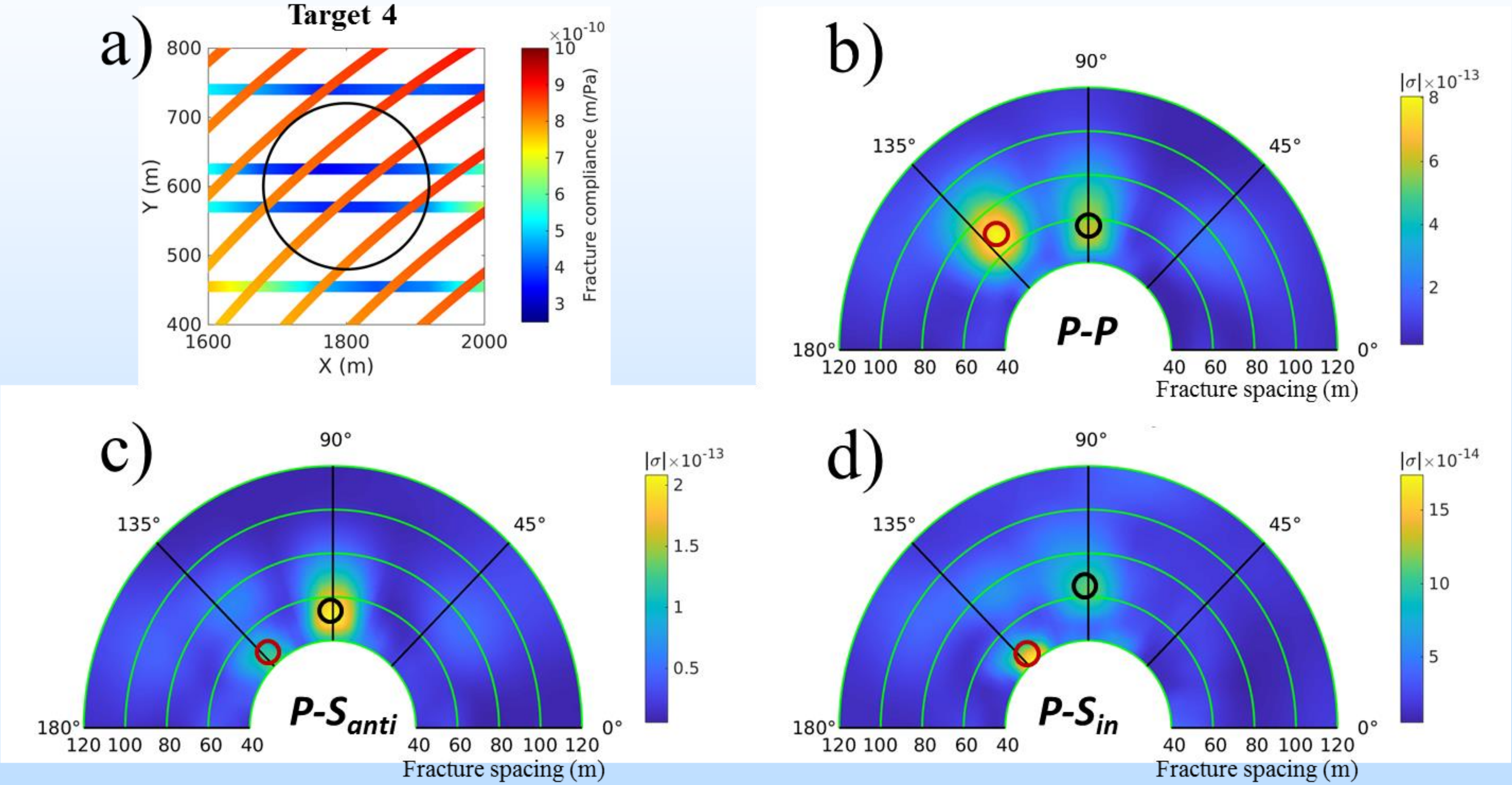

Elastic double-beam neural network (DBNN) machine learning

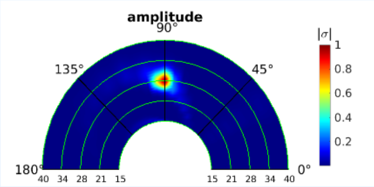

The architecture of our fully-connected neural network including two hidden layers.

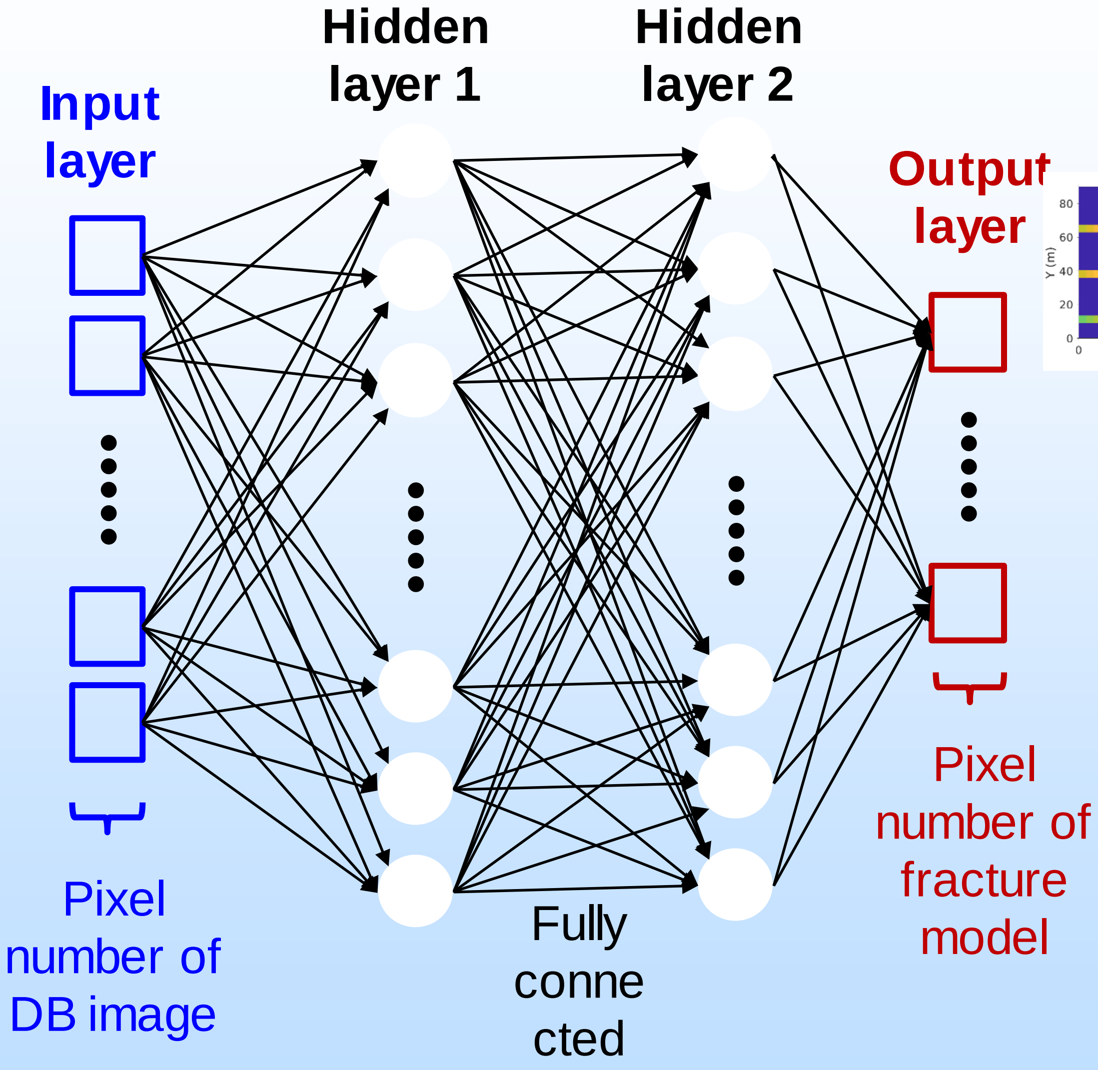

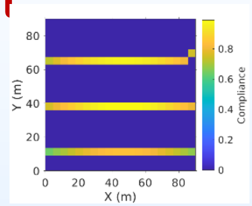

Large-scale faults detected using LANL's new NRU

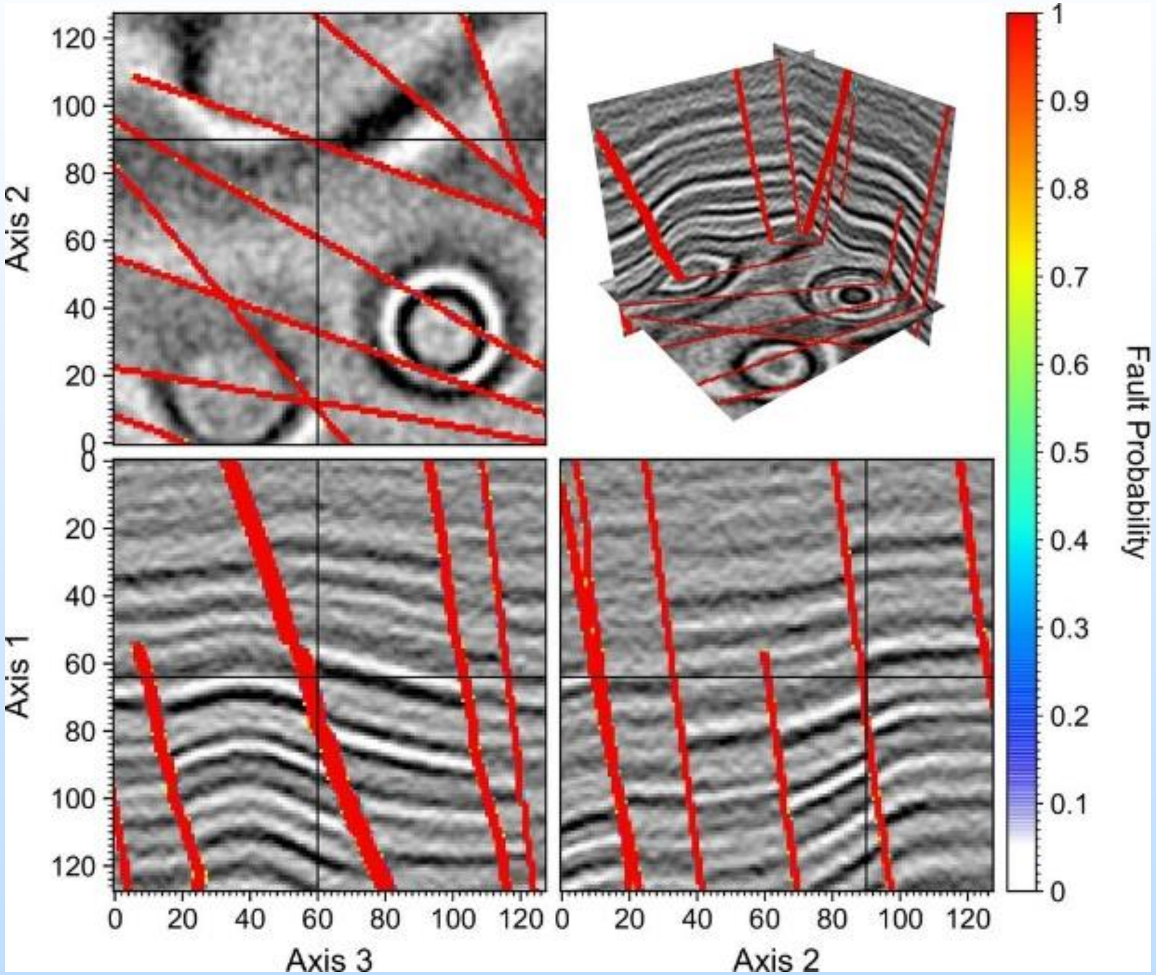

Nested Residual U-shaped convolutional neural network (NRU)

Summary

- Year-1 focused on synthetic model and data tests

- UH, LANL, and Vecta Oil and Gas ltd. worked together and built a 3d seismic model: Vp, Vs, density and spatially varying fracture networks including conjugate fracture sets

- We modeled 3d 9-c shot gathers

- We applied the double-beam method on the modeled datasets and found
  - If there are fractures, DB can invert for the true fractures
  - If there is on fracture in the model, DB reports ‘no fracture’
  - Different frequencies give consistent results → DB method is self verifying

- In the Gigaton CO2 injection scenario, our methods could be extremely useful in providing information: permeable fluid flow pathways, stress state, and earthquake hazards

Acknowledgments

- The work is funded by DOE with funding number DE-FE0032063
- LANL is operated by Triad National Security, LLC, for the U.S. DOE National Nuclear Security Administration (NNSA) under Contract No. 89233218CNA000001. This research used computing resources provided by the LANL Institutional Computing Program supported by the U.S. DOE NNSA under Contract No. 89233218CNA000001.
- We also used computing facilities provided by the UHXfrac group at the University of Houston.
- Vecta Oil and Gas ltd. provided relevant field information